SUPPLEMENTARY INFORMATION
Jiang et al.

Table of Contents

CHEMISTRY	pg 2
CHARGE-REMOTE FRAGMENTATION OF BILE ACID AND GLYCINE CONJUGATE AMPP DERIVATIVES	pg 7
METHOD DEVELOPMENT OF TWO-TIERED LC-MS/MS ASSAY FOR BILE ACID B	pg 10
METHOD VALIDATION OF TWO-TIERED LC-MS/MS ASSAY FOR BILE ACID B	pg 12
SUPPLEMENTAL FIGURES	pg 15
SUPPLEMENTAL TABLES	pg 31

CHEMISTRY

Chemicals and reagents

Deoxycholic acid (DCA, **1**) chenodeoxycholic acid (CDCA, **2**), cholic acid (CA, **3**), α-muricholic acid (**4**), β-muricholic acid (**5**), glycodeoxycholic acid (GDCA, **8**), glycochenodeoxycholic acid (GCDCA, **9**), and glycocholic acid (GCA, **10**), were obtained from Steraloids, Inc. (Newport, RI). N-(3-Dimethylaminopropyl)-N′-ethylcarbodiimide hydrochloride (EDC), 4-(dimethylamino)pyridine (DMAP), diethylamine, acetic acid, N,N-dimethylformamide, acetyl chloride, potassium bis(trimethylsilyl)amide (KHMDS) solution, $LiCuCl_4$ solution, isopentylmagnesium bromide solution, m-chloroperbenzoic acid, dichloromethane, ammonium chloride (NH_4Cl), $RuCl_3$-H_2O, sodium sulfate (Na_2SO_4), N-hydroxysuccinimide, sodium carbonate (Na_2CO_3), p-toluenesulfonic acid monohydrate, *N*,*N*-diisopropylethylamine, acetic anhydride, glycine methyl ester, sodium bicarbonate ($NaHCO_3$), sodium hydroxide (NaOH), hydrochloride solution (HCl), silica gel, dioxane, tetrahydrofuran (THF), ethyl acetate, chloroform, diethyl ether, hexane, Dulbecco's modified Eagle's medium, fetal calf serum, and penicillin G and streptomycin sulfate were obtained from Sigma–Aldrich (St. Louis, MO). Glycine-[$^{13}C_2$,^{15}N], D4-methanol (CD_3OD), D-chloroform ($CDCl_3$), were obtained from Cambridge Isotope (Tewksbury, MA).

Preparation of [7,7,22,22-d4]-3β-(tert-Butyldimethylsilyloxy)cholest-5-ene

A solution of $LiCuCl_4$ (0.1 M solution in THF, 3.62 mL, 0.362 mmol) and [7,7,21,21-d4]-3β-(tert-butyldimethylsilyl)oxy-20-methylpregna-5-en-21-iodide (*40*) (2.03 g, 3.62 mmol), dissolved in THF (15 mL) was cooled to -15°C. An isopentylmagnesium bromide solution (2 M in diethyl ether, 3.62 mL, 7.24 mmol) was added slowly. After further stirring at -15°C for 0.5 h, the reaction mixture was carefully quenched with saturated NH_4Cl (10 mL). The reaction mixture was extracted with dichloromethane (3 x 30 mL). The combined organic layers are washed with saturated brine, dried over Na_2SO_4 and evaporated under reduced pressure. The crude product is purified on a silica gel column using 0 - 10% diethyl ether in hexane to give [7,7,22,22-d4]-3β-(tert-butyldimethylsilanyloxy)cholest-5-ene in 88% yield (1.62 g, 3.21 mmol) ^{1}H NMR (400 MHz, $CDCl_3$): δ 5.29 (d, 1H, J = 2.1 Hz), 3.46 (dddd, 1H, J = 4.9, 4.9, 11.2 and 11.2 Hz), 2.19-2.27 (m, 1H), 2.14-2.18 (m, 1H), 1.99-2.02 (m, 1H), 1.63-1.86 (m, 3H), 1.11-1.62 (m, 17H), 0.97 (s, 3H,), 0.86-0.96 (m, 19H), 0.68 (s, 3H), 0.06 (s, 6H). ^{13}C NMR (100 MHz, $CDCl_3$): δ 146.2, 125.6, 77.2, 61.3, 60.7, 54.7, 47.4, 46.8, 44.4, 44.0, 41.9, 41.1, 40.1, 36.6, 36.3, 32.8, 32.5, 30.5, 28.8, 28.2, 27.4, 27.1, 25.6, 24.0, 23.2, 22.8, 16.4, 0.03

Preparation of [7,7,22,22-d4]-cholestane-3β,5α,6β-triol

To a solution of [7,7,22,22-d4]-3β-(tert-butyldimethylsilyloxy)cholest-5-ene (1.62 g, 3.21 mmol) in dichloromethane (100 ml) was added, by small portions, an excess of *m*-chloroperbenzoic acid (70.1%, 0.95 g, 3.85 mmol) at room temperature. The reaction mixture is stirred overnight at room temperature, washed with aqueous Na_2CO_3, water and brine. After drying over Na_2SO_4, the evaporation of the solvent under reduced pressure affords crude [7,7,22,22-d4]-3β-(tert-butyldimethylsilyloxy)cholestane-5,6-epoxide (two diastereoisomers, α and β- epoxides).

A mixture of above crude product, *p*-toluenesulfonic acid monohydrate (87 mg, 0.321 mmol) in dioxane-water (9:1 v/v; 20 mL) is stirred and heated under reflux for 1.5 h, and evaporated under reduced pressure to dryness. The crude product is purified on a silica gel column using 0 - 10%

methanol in dichloromethane to give impure [7,7,22,22-d4]-cholestane-3β,5α,6β-triol. Recrystallization from chloroform gave pure [7,7,22,22-d4]-cholestane-3β,5α,6β-triol in 60% yield over 3 steps (817 mg, 1.93 mmol). ^{1}H NMR (400 MHz, CD_3OD): δ 3.46 (dddd, 1H, J = 4.9, 4.9, 11.2 and 11.2 Hz), 3.44 (s, 1H), 1.96-2.12 (m, 2H), 1.66-1.95 (m, 3H), 1.24-1.65 (m, 12H), 1.05-1.23 (m, 10H), 0.93 (d, 3H, J = 6.3 Hz,), 0.88 (d, 6H, J = 6.3 Hz), 0.71 (s, 3H). ^{13}C NMR (100 MHz, CD_3OD): δ 76.9, 76.5, 68.4, 57.8, 57.5, 46.6, 44.0, 41.6, 41.5, 40.8, 39.4, 37.1, 33.6, 31.8, 31.5, 29.5, 29.3, 25.3, 24.9, 23.3, 23.1, 22.4, 19.3, 17.4, 12.7.

Preparation of 3β-hydroxy-21,27-dinorcholesta-5,20(22)-dien-26-oic acid methyl ester

(4-Carboxybutyl)triphenylphosphonium bromide (5.12 g, 11.54 mmol) was dissolved in anhydrous THF (30 ml) under a nitrogen atmosphere, and the reaction mixture was cooled to 0ºC. KHMDS in toluene (0.5 M, 57.72 mL, 28.86 mmol) was added dropwise, and the reaction was stirred at 0ºC for 5 minutes. The reaction was then cooled to -40ºC, and (3β,17β)-3-methoxymethoxyandrost-5-ene-17-carboxaldehyde (1.0 g, 2.89 mmol) dissolved in anhydrous THF (30 mL) was added dropwise, and the reaction was stirred at -40ºC for 15 min, and then allowed to slowly warm to room temperature over 1 h. The reaction was then quenched with saturated aqueous NH_4Cl solution and extracted with ethyl acetate (3 x 25 mL). The organic phases were then combined, dried over Na_2SO_4 and concentrated in vacuum. The crude 3β-methoxymethoxy-21,27-dinor cholesta-5,20(22)-dien-26-oic acid was obtained by passing the extract through a column of silica gel (methanol–dichloromethane, gradient elution) and used directly in the next step.

The crude 3β-methoxymethoxy-21,27-dinorcholesta-5,20(22)-dien-26-oic acid was dissolved in methanol (50 mL), and acetyl chloride (2.6 mL) was added dropwise over 1 h. The reaction was then stirred for 16 h at room temperature. Upon completion, the reaction was cooled to 0ºC and neutralized with saturated aqueous $NaHCO_3$, water (50 mL) was added, and the reaction mixture was extracted with dichloromethane (5 x 30 mL). The organic phases were then combined, dried over Na_2SO4 and concentrated *in vacuo*. Column chromatography on silica gel (ethyl acetate–hexane, gradient elution) yielded 3β-hydroxy-21,27-dinorcholesta-5,20(22)-dien-26-oic acid methyl ester as a white solid (1.09 g, 2.45 mmol; 85% over 2 steps). ^{1}H NMR (400 MHz, $CDCl_3$): δ 5.22-5.42 (m, 3H), 3.68 (s, 3H), 3.46 (dddd, 1H, J = 4.9, 4.9, 11.2 and 11.2 Hz), 2.19-2.37 (m, 5H), 1.03-2.18 (m, 21H), 1.02 (s, 3H,), 0.86-0.96 (m, 1H), 0.68 (s, 3H). ^{13}C NMR (100 MHz, $CDCl_3$): δ 174.4, 141.0, 132.4, 129.5, 121.8, 71.9, 56.2, 51.6, 50.5, 48.7, 44.4, 42.4, 37.9, 37.4, 36.8, 33.7, 32.2, 32.1, 31.8, 29.1, 27.1, 25.4, 25.3, 20.9, 19.6, 12.8.

Preparation of 3β-hydroxy-21,27-dinorcholest-5-en-26-oic acid methyl ester

3β-Hydroxy-21,27-dinorcholesta-5,20(22)-dien-26-oic acid methyl ester (133 mg, 0.33 mmol) was dissolved in a 3:1 mixture of THF-water (1 mL) at 0ºC under a nitrogen atmosphere. $RuCl_3$-H_2O (22 mg, 0.083 mmol) was added, followed by the portion-wise addition of $NaBH_4$ (25 mg, 0.66 mmol). The reaction was allowed to slowly warm to room temperature and was stirred 16 h. The reaction was filtered through a small pad of silica, eluting with dichloromethane. The product was then further diluted with dichloromethane (5 mL), and washed with saturated aqueous $NaHCO_3$ (1 mL) then water (1 mL). The organic phases were combined, dried over Na_2SO_4 and concentrated *in vacuo*. The crude 3β-hydroxy-21,27-dinorcholest-5-en-26-oic acid methyl ester (containing a slight amount of $\Delta^{5,6}$ reduced steroid) was then used directly in the next step.

Crude product from the last step (53 mg, 0.124 mmol) was dissolved in formic acid (0.5 mL) by stirring at 75 ºC for 5 min. After the reaction mixture was cooled, 30% H_2O_2 (0.05 mL) was added dropwise. Dichloromethane (0.4 mL) was immediately added, and the reaction mixture was stirred at room temperature for 1h. The dichloromethane was evaporated on a rotary evaporator, and dioxane (0.5 mL) and water (0.75 mL) were added to the residue. The reaction mixture was then refluxed for 16 h. The reaction mixture was evaporated to dryness on a rotary evaporator, and re-dissolved in methanol (2 mL). To the mixture was added NaOH (13 mg, 0.32 mmol) and the reaction mixture was stirred 2 h at room temperature. The reaction mixture was neutralized with formic acid and the reaction was evaporated to dryness to give the crude 3β-hydroxy-21,27-dinor cholest-5-en-26-oic acid as a white residue.

The crude 3β-hydroxy-21,27-dinorcholest-5-en-26-oic acid was suspended in methanol (5 mL), and acetyl chloride (0.25 mL) was added dropwise. The reaction mixture was allowed to stir for 1h. The reaction was cooled to 0ºC, and neutralized with saturated aqueous $NaHCO_3$. The reaction mixture was diluted with water (5 mL) and was extracted with dichloromethane (5 x 5 mL). The organic phases were combined, dried over Na_2SO_4, and concentrated *in vacuo*. The residue was purified by column chromatography on silica gel (methanol–dichloromethane, gradient elution), to yield 3β-hydroxy-21,27-dinorcholest-5-en-26-oic acid methyl ester as a white solid (34.0 mg, 0.8 mmol, 60% yield over 3 steps).^{1}H NMR (300 MHz, $CDCl_3$): δ 5.35 (d, 1H, J = 6.0), 3.67 (s, 3H), 3.53 (m, 1H), 2.18-2.34 (m, 4H), 0.90-2.06 (m, 27H), 1.01 (s, 3H,), 0.57 (s, 3H). ^{13}C NMR (75 MHz, $CDCl_3$): δ 174.6, 141.0, 121.8, 71.9, 56.3, 51.6, 51.0, 50.7, 42.4, 42.1, 38.0, 37.5, 36.8, 34.3, 32.2, 32.1, 31.8, 30.2, 29.8, 28.6 (x2), 25.1, 24.9, 21.0, 19.6, 12.5.

Preparation of 3β,5α,6β-trihydroxy-21,27-dinorcholest-5-en-26-oic acid

3β-Hydroxy-21,27-dinorcholest-5-en-26-oic acid methyl ester (34.0 mg, 0.078 mmol) was dissolved in a 4:1 mixture of dioxane-water (1.25 mL) and NaOH (6 mg, 150 mmol) was added. The reaction was stirred overnight at 40ºC and quenched with 1N HCl, and the solvents were evaporated. The remaining solids were washed with water (1 mL x 3). The remaining solid was recrystallized in a 1:1 mixture of warm methanol-dichloromethane to yield 3β,5α,6β-trihydroxy-21,27-dinorcholest-5-en-25-oic acid as colorless crystals in 90% yield (29.6 mg, 0.0702 mmol). ^{1}H NMR (300 MHz, DMSO-d6): δ 3.79 (m, 1H), 3.64 (br s, 1H,), 2.17 (d, 2H, J = 6.4 Hz), 1.03-1.92 (m, 23H), 1.03 (s, 3H,), 0.86-0.96 (m, 3H), 0.53 (s, 3H). ^{13}C NMR (75 MHz, DMSO-d6): δ 174.4, 74.3, 74.1, 65.7, 55.2, 50.4, 45.0, 41.8, 40.9, 37.9, 37.7, 34.6, 33.7, 32.0, 31.1, 29.9, 29.7, 29.0, 28.1, 27.9, 24.5, 24.2, 20.4, 16.2, 12.4.

Preparation of bile acid A N-hydroxysuccinimide ester

Bile acid A (0.62 g, 1.52 mmol) was dissolved in a mixture of dioxane (15 mL) and dichloromethane (15 mL) and 1-ethyl-3-(3-dimethylaminopropyl)carbodiimide (1.41 g, 9.10 mmol) was added. N-hydroxysuccinimide (1.05 g, 9.10 mmol) was then added and the reaction was stirred 16 h at 35ºC. Upon reaction completion, the reaction mixture was loaded directly onto a silica gel column, and purified using methanol–dichloromethane, gradient elution, to yield the bile acid A N-hydroxysuccinimide ester in 66% yield (0.50 mg, 0.99 mmol). ^{1}H NMR (400 MHz, $CDCl_3$:CD_3OD; 5:1) δ 2.77 (m, 4H, succinate), 1.06 (s, 3H), 0.87 (d, 3H, J = 6.4 Hz), 0.70 (s, 3H); ^{13}C NMR (100 MHz, $CDCl_3$:CD_3OD, 2:1) δ 172.9 169.9, 169.4, 75.8, 75.4, 67.3, 55.9,

55.7, 45.4, 42.8, 39.9, 38.1, 35.2, 34.0, 32.3, 30.6, 30.3, 30.3, 28.1, 27.9, 25.6 (x 2), 25.5, 24.1, 21.1, 18.1, 16.6.

Preparation of N-(3β,5α,6β)-3,6-Diacetoxy-5-hydroxy-cholan-24-oyl)glycine methyl ester

Bile acid A *N*-hydroxysuccinimide ester (2.08 g, 4.1 mmol) was dissolved in anhydrous THF (200 mL). *N*,*N*-diisopropylethylamine (2.9 mL, 16.45 mmol) was added, followed by glycine methyl ester (0.77 g, 6.2 mmol) and the reaction was stirred 16 h at room temperature, and the reaction mixture was then concentrated *in vacuo*, to give the 2.5 g of crude *N*-(3β,5α,6β-trihydroxycholan-24-oyl)glycine methyl ester.

At this point, *N*-(3β,5α,6β-trihydroxycholan-24-oyl)glycine methyl ester was found to be difficult to separate from impurities due to both poor solubility, and byproducts with overlapping retention times from a column. Therefore, *N*-(3β,5α,6β-trihydroxycholan-24-oyl)glycine methyl ester was acetylated as part of the purification process. Accordingly, a portion of the impure *N*-(3β,5α,6β-trihydroxycholan-24-oyl)glycine methyl ester (2.5 g, 5.2 mmol) was dissolved in pyridine (40 mL) and 4-dimethylaminopyridine (327 mg, 2.6 mmol) was added, followed by acetic anhydride (4.0 mL, 41.8 mmol). After 16 h at room temperature, the pyridine was evaporated under vacuum, and the reaction was re-dissolved in dichloromethane (75 mL) and washed with water (30 mL), 1 N HCl (30 mL), water (30 mL), saturated aqueous $NaHCO_3$ solution (30 mL), and water (30 mL). The organic layer was concentrated *in vacuo*, and the residue was purified by column chromatography on silica gel (methanol–dichloromethane, gradient elution), to yield *N*-(3β,5α,6β)-3,6-diacetoxy-5-hydroxy-cholan-24-oyl)glycine methyl ester in 73% yield (1.7 g, 3.0 mmol). ^{1}H NMR (400 MHz, $CDCl_3$) δ 6.53 (t, 1H, J = 5.6 Hz), 5.05 (m, 1H), 4.64 (br s, 1H), 3.92 (t, 2H, J = 5.4 Hz), 3.65 (s, 3H, OCH_3), 2.98 (s, 1H), 1.98 (s, 3H), 1.92 (s, 3H), 1.05 (s, 3H), 0.83 (d, 3H, J = 6.4 Hz), 0.59 (s, 3H); ^{13}C NMR (100 MHz, $CDCl_3$) δ 174.1, 170.8, 170.7, 170.3, 76.2, 74.4, 70.9, 56.0, 55.7, 52.2, 44.7, 42.7, 41.1, 39.9, 38.3, 36.5, 35.5, 33.1, 31.8, 31.6, 31.3, 30.7, 28.1, 26.6, 24.0, 21.5, 21.4, 21.0, 18.3, 16.3, 12.2.

Preparation of bile acid B

N-(3β,5α,6β)-3,6-Diacetoxy-5-hydroxy-cholan-24-oyl)glycine methyl ester (1.03 g, 1.83 mmol) was dissolved in a mixture of methanol (50 mL) and water (50 mL). Crushed NaOH (4.0 g, 100 mmol) was added and the reaction was stirred at 40ºC for 16 h. Upon completion, the solvents were evaporated under vacuum, and the reaction contents were heated in hot methanol, and the remaining insoluble solids were filtered. This step was repeated 2 more times on the remaining solids to ensure the majority of the steroid was dissolved. The filtrates were combined and concentrated to give bile acid B as a white solid in quantitative yield (0.85 g, 1.83 mmol). mp 259-261ºC (from methanol); IR: 3274, 2918, 2863, 1713, 1651, 1594, 1403, 1036 cm^{-1}; ^{1}H NMR (400 MHz, CD_3OD) δ 4.01 (m, 1H), 3.76 (s, 2H), 3.45 (s, 1H), 2.36-2.25 (m, 1H), 2.10-2.19 (m, 2H), 1.90-2.10 (m, 2H), 1.21-1.90 (m, 16H), 1.05-1.21 (m, 7H), 0.97 (d, 3H, J = 5.2 Hz), 0.72 (s, 3H); ^{13}C NMR (100 MHz, CD_3OD) δ 176.5, 175.9, 76.8, 76.5, 68.3, 57.4, 57.4, 46.5, 44.0, 44.0, 41.5 (x2), 39.3, 36.9, 35.3, 34.0, 33.5, 33.1, 31.7, 31.6, 29.2, 25.2, 22.3, 18.9, 17.3, 12.6.

Preparation of N-(3β,5α,6β)-3,6-diacetoxy-5-hydroxy-cholan-24-oyl)glycine-[$^{13}C_2$,^{15}N] methyl ester

Bile acid A N-hydroxysuccinimide ester (1.5 g, 2.97 mmol) was dissolved in anhydrous THF (150 mL) and *N*,*N*-diisopropylethylamine (2.1 mL, 11.87 mmol) was added. Glycine-[$^{13}C_2$,^{15}N] (0.57 g, 4.45 mmol) was dissolved in water (15 mL) and added to the reaction flask. The reaction was stirred vigorously for 10 min (or until reaction becomes a clear homogenous mixture). The reaction was then stirred an additional 16 h at room temperature. Solvents were then evaporated under vacuum, and the reaction contents were re-dissolved in hot THF and the insoluble solids were filtered off, and the filtrate was concentrated to give crude bile acid B-[$^{13}C_2$,^{15}N]. The impure bile acid B-[$^{13}C_2$,^{15}N] (200 mg, 0.43 mmol) was then re-dissolved in methanol (50 mL) and cooled to 0 ºC. Acetyl chloride (2.5 mL) was added dropwise. After 10 min at 0ºC, the reaction was brought to room temperature and stirred 16 h. Upon completion, the reaction was cooled to 0ºC and was carefully neutralized with saturated aqueous $NaHCO_3$ solution followed by adding water (50 mL). The reaction mixture was extracted with dichloromethane (4 x 50 mL) and concentrated *in vacuo*. The crude glycine-[$^{13}C_2$,^{15}N] methyl ester was re-dissolved in pyridine (10 mL) and 4-dimethylaminopyridine (26 mg, 0.21 mmol) was added, followed by acetic anhydride (0.34 mL, 3.42 mmol). After 16 h at room temperature, the pyridine was evaporated under vacuum, and the reaction was re-dissolved in dichloromethane (30 mL) and washed with water (10 mL), 1 N HCl (10 mL), water (10 mL), saturated aqueous $NaHCO_3$ solution (10 mL), water (10 mL). The organic layer was concentrated *in vacuo*, and the residue was purified by column chromatography on silica gel (methanol–dichloromethane, gradient elution), to yield *N*-(3β,5α,6β)-3,6-diacetoxy-5-hydroxy-cholan-24-oyl)glycine-[$^{13}C_2$,^{15}N] methyl ester in 64% yield (157 mg, 0.28 mmol). ^{1}H NMR (400 MHz, $CDCl_3$) δ 6.07 (d, 1H, J = 9.4 Hz), 5.14 (m, 1H), 4.70 (s, 1H), 4.21 (br s, 1H), 3.86 (br s, 1H), 3.75 (d, 3H, J = 3.6 Hz, OCH_3), 2.06 (s, 3H), 2.01 (s, 3H), 1.14 (s, 3H), 0.92 (d, 3H, J = 6.4 Hz), 0.68 (s, 3H); ^{13}C NMR (100 MHz, $CDCl_3$) δ 174.1, 173.9, 171.2 (^{13}C), 170.6 (^{13}C), 76.3, 74.8, 71.0, 56.1, 55.8, 52.5, 44.9, 42.9, 41.7 (^{13}C), 41.5 (^{13}C), 41.0 (^{13}C), 40.9 (^{13}C), 40.0, 38.5, 36.8, 35.6, 33.4, 33.3, 31.9, 31.7, 31.4, 30.8, 28.3, 26.8, 24.2, 21.6, 21.6, 21.1, 18.5, 16.4, 12.3

Preparation of bile acid B-[$^{13}C_2$,^{15}N]

N-(3β,5α,6β)-3,6-Diacetoxy-5-hydroxy-cholan-24-oyl)glycine-[$^{13}C_2$,^{15}N] methyl ester (157 mg, 0.28 mmol) was dissolved into a mixture of methanol (5mL) and water (5mL), crushed NaOH (0.5 g, 12.5 mmol) was added, and the reaction was stirred at 40ºC for 16 h. Upon completion, the solvents were evaporated under vacuum, and the reaction contents were heated in hot methanol, and the remaining insoluble solids were filtered. This step was repeated 2 more times on the remaining solids to ensure the majority of the steroid was dissolved. The filtrates were combined and concentrated to give bile acid B as a white solid in 70% yield (91 mg, 0.19 mmol). mp 275-277ºC; IR: 3391, 2936, 2867, 1629, 1551, 1376, 1042 cm^{-1}; ^{1}H NMR (400 MHz, CD_3OD) δ 4.01 (m, 1H), 3.91 (d, 1H, J = 5.6 Hz), 3.56 (d, 1H, J = 5.2 Hz), 3.45 (br s, 1H), 2.36-2.25 (m, 1H), 2.10-2.19 (m, 2H), 1.90-2.10 (m, 2H), 1.21-1.90 (m, 16H), 1.05-1.21 (m, 7H), 0.97 (d, 3H, J = 6.4 Hz), 0.72 (s, 3H); ^{13}C NMR (100 MHz, CD_3OD) δ 177.0 (^{13}C), 176.7, 176.4 (^{13}C), 176.3, 76.8, 76.5, 68.3, 57.4, 57.4, 46.5, 44.9 (^{13}C), 44.8 (^{13}C), 44.3 (^{13}C), 44.2 (^{13}C), 44.0 (^{13}C), 41.5, 41.4, 39.3, 37.0, 35.3, 33.5, 33.1, 31.7, 31.6, 29.2, 25.2, 22.3, 18.9, 17.3, 12.6.

CHARGE-REMOTE FRAGMENTATION OF BILE ACID AND GLYCINE CONJUGATE AMPP DERIVATIVES

Shown in **Figure S2 and S13** are the product ion spectra of standard bile acid AMPP derivatives studied. The diagnostically significant fragment ions are presented in **Table S1 - 5**. In addition to the two major fragment ions present at m/z 169 (fragment **T**) and m/z 183 (fragment **S**) arising from AMPP tag, tandem mass spectra of AMPP-derivatized bile acids demonstrated less abundant but informative fragment ions result from cleavages of ring systems and side chains of bile acids. The structures of fragments S and T have been proposed by Yang et al (*42*).

Fragmentation of AMPP derivatives of unconjugated bile acids (1-7)

The HCD spectra (**Figure S2; Table S1, S3-S4**) of all unconjugated bile acid AMPP derivatives showed ions formed by neutral loss of 18 Da (fragment **A**, - H_2O), 32 Da (fragment **B**, - CH_3OH), while only some AMPP derivatives produce product ions from loss of 34 Da (fragment **D**, - CH_3OH - H_2), 36 Da (fragment **E**, - $2H_2O$), 50 Da (fragment **C**, - H_2O - CH_3OH), 52 Da (fragment **F**, - CH_3OH - H_2O - H_2), 68 Da (fragment **G**, -$2H_2O$ - CH_3OH) (**Figure S3**). The fragment **B** resulting from loss of CH_3OH probably involving the participation of the 19-methyl and 3-hydroxyl groups via cleavage of the bond between C-4 and C-5 (**Figure S3**, route a). This ion is present in the spectra of all bile acids (**1**-**7**) examined, indicating its utility for diagnosis of 3-hydroxyl group in these compounds. The double bond formed between C5 and C10 in fragment **B** probably encourages C8-C9 bond fragmentation by a retro Diels Alder reaction (**Figure S3**, route b); and the subsequent hydrogen rearrangement leads to fragment **H** by cleaving the bond between C-13 and C-17 that eliminates the A and B rings. Fragment **H** in CDCA (**2**), CA (**3**), α-muricholic acid (**4**), β- muricholic acid (**5**), 5β-cholanic acid-3α,4β,7α-triol (**6**) retains the 7-hydroxyl group, and thus, can be used to assign the 7-hydroxyl group.

The fragmentations at ring junctions provide important information to locate the substituents on the steroid ring (**Figure S4**). A retro-cycloaddition mechanism accounts for formation of Fragments **I** (**Figure S4**, route a), **J** (**Figure S4**, route b) and **K** (**Figure S4**, route c), and bile acid isomers differed in the position of the hydroxyl group can be differentiated. The DCA (**1**), CDCA (**2**), CA (**3**), α-muricholic acid (**4**), β- muricholic acid (**5**), 5β-cholanic acid-3α,4β,7α-triol (**6**) bear no hydroxyl group on the D ring and side chain, and all form a common Fragment **K** at *m/z* 349. DCA (**1**) and CA (**3)** also contain a hydroxyl group on C ring and give rise to **J** ion of *m/z* 419. In contrast, α/β-muricholic acid (**4**/**5)** and 5β-cholanic acid-3α,4β,7α-triol **6** yielded m/z 403 due to the absence of hydroxyl group on C ring. Both CA (**3)** and α/β-muricholic acid (**4**/**5)** gave fragment **I** at *m/z* 503 due to the presence of 2 hydroxyl groups on B and C rings, while CDCA (**2**) and 5β-cholanic acid-3α,4β,7α-triol (**6)** yielded **I** ion at *m/z* 487 due to only 1 hydroxyl group is present on B and C rings. Introduction of a hydroxyl group at C-5 in 21,26,27-trinorcholestan-25-oic acid-3β,5α,6β-triol (**7**) inhibited the cleavage at A/B ring and prevented **I** ion formation. The lack of **I** ion is characteristic of 5-hydroxylation.

Rupture of D-ring in the AMPP derivative of bile acids **1**-**6** involving hydrogen rearrangement and cycloelimination gave rise to **L** ion at *m/z* 309, and its subsequent fragment **M** ion at *m/z* 293 formed by loss of a methane involving H-transfer via six-membered ring intermediate (**Figure**

S5). The cleavage of D-ring of compound **7** gave fragment **L´**at *m/z* 323 and a fragment **M´**at *m/z* 309 that was formed via cycloelimination (**Figure S5**).

Bile acids **1 - 6** are naturally occurred and possess a common 5 carbons branched side chain at position 17 of the steroid core. Ions at *m/z* 267 (fragment **N**), 239 (fragment **O**), 211 (fragment **P**), and 226 (fragment **Q**), from charge-remote fragmentation (CRF) were observed. We propose that fragments **N** (**Figure S6**, route a), **O** (**Figure S6**, route b), **P** (**Figure S6**, route c) and **S** (**Figure S**7 route b) arise from 1,4-hydrogen elimination; while ions of **Q** (**Figure S**7, route a) and **T** (**Figure S**7, route c) are formed by hemolytic cleavage. The cyclization of **Q** ion and subsequent elimination of a hydrogen radical and methyleneamine gave fragment **R** (**Figure S**7). The 21,26,27-trinorcholestan-25-oic acid-3β,5α,6β-triol (**7)** has a straight 6-carbon side chain at position 17 of steroid core, which underwent the similar fragmentations to yield **N** and **O** ions at *m/z* 281, 253, respectively (**Table S1**).

Fragmentation of AMPP derivatives of glycine conjugated bile acids (8-10)

Glycine conjugated bile acid AMPP derivatives of **8 -10** also yielded informative ions in HCD mode via CRF (**Figure S2** and **Table S5**). The ions arising from losses of 18 Da (fragment **GA**, - H_2O) and of 32 Da (fragment **GC**, - CH_3OH, **Figure S8**, route a) were again observed in derivatives of **8 -10**, but the ion from loss of 36 Da (fragment **GB**, - $2H_2O$) was only observed in derivative of **8** (**Figure S8**). The retro Diels Alder reaction in fragment **GC** cleaves C8-C9 bond (**Figure S8**, route b), and subsequent hydrogen rearrangement and cleavage of the bond between C-13 and C-17 leads to fragment **GH**. The 7-hydroxyl group in GCDCA (**9**) and GCA (**10**) was intact in **GH**, characteristic to the 7-hydroxyl group. The cleavages at A/B, B/C, C/D ring junctions via retro-cycloaddition mechanism yielded fragments **GF** (**Figure S9**, route a), **GG** (**Figure S9**, route b), and **GI** (**Figure S9**, route c), respectively. Hydrogen rearrangement (**Figure S10**, route a) and elimination (**Figure S10**, route b) of D-ring in derivatives of **8-10** gave rise to **GK** and **GJ** ions at *m/z* 366 and *m/z* 352, respectively. The **GK** ion of *m/z* 366 eliminates a methane to form **GL** ion at *m/z* 350, and an ethane to form **GM** ion at *m/z* 336, following 1,3-H shift. These losses of methane and of ethane are postulated to proceed via six-membered ring transition state (**Figure S10**). Alternatively, loss of a hydrogen from **GJ** ion also gives **GL** ion.

Side chain cleavages from glycine conjugated bile acid-AMPP derivatives provide not only the structural information available for the unconjugated counterparts, but also the information unique to the acyl glycine moiety of the compounds. **GV** (**Figure S11**, route g) and **GW** ions (**Figure S11**, route h) at *m/z* 183 and 169 are equivalent to **S** and **T** ions, respectively. We propose the similar fragmentation processes to as shown in **Figure S7** for formation of ions of **GN** (*m/z* 324, **Figure S11**, route a), **GO** (*m/z* 296, **Figure S11**, route b), and **GP** (*m/z* 268, **Figure S11**, route c) through 1,4-hydrogen elimination. The 1,4-hydrogen elimination involving the side chain leads to **GQ** at *m/z* 211 (**Figure S11**, route d) and **GR** at *m/z* 240 (**Figure S11**, route e). We also propose that **GR** eliminates an isocyanic acid to yield **GS**, involving a rearrangement process to 1,4-Dihydro-3(2H)-isoquinolone followed by retro Diels Alder reaction and cyclization. Elimination of H_2 from **GS** gives rise to **GT**. A major ion (fragment **GU**) at *m/z* 185 probably results from β-elimination (**Figure S11**, route f).

The glycine moiety can likely be eliminated as aziridinone to give fragment **GX**, which is corresponding to the unconjugated bile acid-AMPP derivative. Further loss of one and two

waters from **GX** yields **GY** and **GZ**, respectively (**Figure S12**). However, the further ring and side chain fragmentation from **GX** was not observed due to low abundance of **GX**. The elimination of aziridinone may involve rearrangement of amides and subsequent nucleophilic attack of released amino group on the glycine amide (**Figure S12**, route a). A loss of CO to **GAA** from **GA** was also observed, probably involving the glycine moiety. The final product ion of **GAB** may arise from **GAA** by loss of a pyridine (**Figure S12**, route b).

Fragmentation of AMPP derivatives of bile acid A and B

The HCD spectrum of bile acid A-AMPP derivative is dominated by **T** ion at *m/z* 169 and **S** ion at *m/z* 183 arising from AMPP tag (**Figure S13A**). **B** ion at *m/z* 543 arose from loss of methanol, suggesting that a 3-hydroxyl group is attached to A ring. The observation of **K** ion at *m/z* 349 indicates the absence of hydroxyl group on D ring and side chain. This notion is also confirmed by the presence of **L** (*m/z* 309) and **M** (*m/z* 293) ions arising from cleavage of D ring, as well as **N** (*m/z* 267), **O** (*m/z* 239), **P** (*m/z* 211), **Q** (*m/z* 226), and **R** (*m/z* 196) ions from various cleavages of the side chain. The **J** ion at m/z 403 points to the absence of hydroxyl group on C ring; and the **H** ion at *m/z* 375 rules out the presence of the hydroxyl group at C-7 of B ring. The lack of **I** ion suggests the existence of 5-hydroxyl group. The ions corresponding to neutral loss of 18 Da (fragment **A**, - H_2O), 32 Da (fragment **B**, - CH_3OH), 34 Da (fragment **D**, - CH_3OH - H_2), 36 Da (Fragment **E**, - $2H_2O$), 50 Da (Fragment **C**, - H_2O - CH_3OH), 52 Da (Fragment **F**, - CH_3OH - H_2O - H_2), and 68 Da (fragment **G**, -$2H_2O$ - CH_3OH) were also observed (**Table S1**). The bile acid A is temporarily assigned as 5α-cholanic acid-3β,5α,6β-triol.

The HCD spectrum of the M^+ ion of bile acid B AMPP-derivative at m/z 632 contains prominent **GW** ion at *m/z* 169, together with **GU** at *m/z* 185 and **GV** at *m/z* 183 arising from AMPP tag (**Figure S13B**). The elimination of aziridinone to yield fragment **X** at *m/z* 575 indicates the presence of glycine conjugate. Other fragments that are characteristics of glycine conjugate include fragments **GP** (*m/z* 268), **GQ** (*m/z* 211), **GR** (*m/z* 240), **GS** (*m/z* 197), **GT** (*m/z* 195), **GY** (*m/z* 586), and **GZ** (*m/z* 507). The presence of **GC** ion at m/z 600 (loss of methanol) suggests the attachment of a 3-hydroxyl group on A ring; and **GI** ion observed at *m/z* 406 also rules out the presence of a hydroxyl group on D ring and side chain. Ions at *m/z* 352 (**GJ**), *m/z* 366 (**GK**), *m/z* 350 (**GL**) and *m/z* 336 (**GM**) from rupture of D ring, and ions at *m/z* 324 (**GN**) and *m/z* 296 (**GO**) from side chain cleavages also confirm that hydroxyl group is absent on D ring and side chain. The ions observed at *m/z* 460 (**GG**) and *m/z* 432 (**GH**) reflect that there is no hydroxyl group on C ring, and the presence of 5-hydroxyl group due to lack of **GF** ion. The feature ions corresponding to losses of 18 Da (fragment **GA**, - H_2O), 36 Da (fragment **GB**, - $2H_2O$), 34 Da (fragment **GD**, - CH_3OH - H_2), 50 Da (fragment **GE**, - H_2O - CH_3OH), 44 Da (fragment **GAA**, - H_2O - CO), and 125 Da (fragment **GAB**, - H_2O – CO - pyridine) were also observed (**Table S2**). Collectively, the structure of the bile acid A is temporarily assigned as 5α-cholanic acid-3β,5α,6β-triol N-(carboxymethyl)-amide.

METHOD DEVELOPMENT OF TWO-TIERED LC-MS/MS ASSAY FOR BILE ACID B

Selection of matrix for calibration and quality control samples

Ideally, the matrix for calibration and quality control (QC) dried blood spot samples is bile acid B free blood to which accurately known concentration of the bile acid B can be spiked. Many normal newborn dried blood spots were found with negligible levels of bile acid B, suggesting that blood from normal neonate is an ideal matrix for calibration and QC dried blood spot samples. We screened umbilical cord bloods from normal neonates and found that bile acid B in most of them was undetectable. In addition, we found that the red blood cells from adult donors contained no bile acid B. As freshly drawn umbilical cord blood may not always be available, we prepared blood with hematocrit of 55% by mixing plasma from umbilical cord blood and fresh red blood cells from adult donor. This artificial blood was used as matrix for calibration and QC dried blood spot samples. When calibration and QC samples in blood were prepared in polypropylene containers, part of bile acid B was lost due to non-specific binding to the container surface. The absorption loss was not found in regular glass container, thus the calibration and QC samples were prepared in glass containers before spiking to newborn screening cards.

Sample preparation

A two-step extraction was used in dried blood spot sample preparation. First, the internal standard (bile acid $B^-[^{13}C_2,^{15}N]$) in aqueous solution was added to the dried blood spot disk to dissolve the dried blood into the aqueous phase, followed by the addition of acetonitrile to precipitate proteins that were eluted from the dried blood spot cards. The internal standard working solution contains 1% sodium dodecyl sulfate (SDS) and 50 mM trisodium citrate at pH 12. The SDS was used to prevent nonspecific binding of the bile acid B and internal standard to the plastic surface, and citrate under basic condition can release bile acid B from ionic interaction with iron of hemoglobin and improve the extraction recovery. The SDS was eluted before bile B, did not cause matrix effect to bile acid B, and did not contaminate the mass spectrometer ion source. We did not observe any significant sensitivity loss after analysis of more than 6500 samples. The extraction was performed in 96 well plates, and application of a 96 channels pipette to add internal standard and transfer extracts allows preparation of several hundreds of samples a day.

LC-MS/MS method

The electrospray ionization mass spectrometry detection for bile acid B and its internal standard (bile acid $B^-[^{13}C_2,^{15}N]$) was examined extensively. While weak $[M+H]^+$ ions were observed in positive ionization mode, the deprotonated molecular ions $[M-H]^-$ were the predominating ion in negative ionization mode, thus, $[M-H]^-$ ions were used for further LC-MS/MS method development. The collision-induced dissociation (CID) of $[M - H]^-$ ion produced only one product ion corresponding to deprotonated glycine. MRM mode was used to detect bile acid B and its internal standard by monitoring the transitions *m/z* 464→*m/z* 74 and *m/z* 467→*m/z* 77, respectively.

The bile acid B under basic mobile phase conditions showed the highest sensitivity, but basic pH mobile phase significantly shortened lifetime of most reversed phase columns. ACE Excel Super C18 column with working pH range of 1.5-11.5 was chosen to separate bile acid B from

interferences. To further improve column robustness, diethylamine - hexafluoro-2-propanol buffer at pH 8.9 was used as mobile phase. The column under our condition was highly robust, and no significant changes in retention time, resolution, and peak shape were found after more than 6500 samples were analyzed.

METHOD VALIDATION OF TWO-TIERED LC-MS/MS ASSAY FOR BILE ACID B

To assess the performance of the method for the quantification of bile acid B, a series of validation experiments was performed to address all FDA recommendations for bioanalytical method validation, as well as testing several additional variables of the dried blood spot technique (*22, 23*). The validation assessment considered the following: sensitivity, selectivity, accuracy, precision, linearity, carry-over, recovery, matrix effect, effect of spotting volumes, effect of hematocrit, effect of punch location, and stabilities in whole blood, dried blood spots, processed samples, and stock solutions.

Sensitivity

The lower limit of quantification (LLOQ) is defined as the lowest concentration that can be determined with suitable accuracy and precision, typically less than 20% relative error (RE) and 20% CV for LC–MS/MS assays, in the biological matrix. During the method validation experiments, the lowest calibration standard for the bile acid B was set at 5 ng/mL. This concentration could be measured with a signal/noise ratio greater than 5:1, and the acceptable precision (≤10% CV) and accuracy (within ±9% RE) for bile acid B were obtained under both short and long LC conditions (**Tables S8**)

Selectivity

Although bile acid B is an endogenous analyte, its level in most normal newborn dried blood spot samples is undetectable. This conclusion was drawn by the analysis of 36 control newborn dried blood spot samples. All the samples demonstrated no significant interference (as defined by having no peak with an area greater than 20% of the LLOQ calibration standard for bile acid B or no greater than 5% for the internal standard). The selectivity of the assay was further confirmed by evaluating plausibly interfering bile acids (glycocholic acid and glycomuricholic acid), and the resulting chromatograms demonstrated no interference at the retention time of bile acid B.

Accuracy and precision

The accuracy and precision of the method were evaluated by analyzing six replicates of QC samples at lower limit (10 ng/mL (LLQC), low (30 ng/ml, LQC), medium (150 ng/ml, MQC) and high level (300 ng/ml, HQC) QC samples in three separate batches (n = 6 per batch) against a calibration curve. A summary of the intra-and inter-batch precision and accuracy data of individual QC concentrations for bile acid B is shown in **Tables S8**. For short LC condition, the precision was less than 15% CV and the accuracy was in the range of ±15% RE over the three concentration levels evaluated in all three batches (**Table S8**). Similar precision and accuracy were also obtained from these batches under long LC condition (**Table S8**). These results indicated that satisfactory precision and accuracy could be achieved.

Linearity

The calibration range was 5–500 ng/mL for all three batches. The response was linear, and the r^2 values for the three batches were more than 0.99.

Carryover

In order to evaluate carryover, a blank dried blood disk extract was analyzed immediately after the upper limit of quantification (ULOQ, 500 ng/mL) sample. Under both short and long LC conditions, no peaks around the same retention time of bile acid B was observed in the chromatogram of the blank matrix sample analyzed immediately after ULOQ. As a result, carryover from previous concentrated samples up to 500 ng/mL of bile acid B is judged to be negligible.

Recovery and matrix effect

The recovery and matrix effect were evaluated by preparing (A) extracts of whole area of LQC and HQC dried blood spot (5 µl of blood); (B) extracts of whole area of blank dried blood spot (5 µl of blood) post-fortified with both the bile acid B and the internal standard with the concentrations the same as in (A); and (C) neat solutions with the concentrations of the bile acid B and the internal standard the same as in (A) and (B). The recovery and matrix factor were assessed by comparing the peak area of (A) and (B), (B) and (C), respectively. The recoveries of bile acid B and internal standard are 96% and 91%, respectively. The matrix factors of 1.06 and 1.09 were obtained for bile acid B and internal standard, respectively. A matrix factor value of close to one indicates minimum ionization suppression or enhancement. Furthermore, the internal standard normalized matrix factor is also close to one, suggesting that the matrix effect on analysis of bile acid B in dried blood spot was minimal.

Effect of spotting volumes

Owing to the potential difficulties arising when trying to accurately spot blood in a clinical sampling environment, the effect of spot volume was assessed at LQC and HQC levels in triplicate by spotting different volumes (50, 75, 100 µL) of blood on newborn screening cards. The spot areas of 50, 75, 100 µL of blood are slightly smaller, slightly bigger and significantly bigger than the cycle on newborn screening card, respectively. The bile acid B concentrations of these dried blood spots were quantified against a standard curve with 50 µL spotting volume. Acceptance criteria were mean difference to nominal value within ±15%. The relative errors of all the QC samples with different spotting volumes were within ±5%. The precision (%CV) for all spot volume measurements were < 8%. Therefore, dried blood spots with spotting volume in the range of 50 to 100 µl can be accurately quantified with standard curve prepared with spotting volume of 50 µL.

Effect of hematocrit

Hematocrit level is directly proportional to blood viscosity. It affects flux and diffusion properties of the blood spotted on the newborn screening card. A higher viscosity leads to smaller size of blood spot formed and affects spot homogeneity. Variations in hematocrit can also lead to differences in analyte recovery and varying matrix effects. The normal newborn hematocrit ranges from 42 to 65% (*41*). We tested LQC and HQC dried blood spots with five hematocrit levels (40%, 50%, 55%, 60%, and 70%) in triplicate to evaluate whether the accuracy would be affected. The bile acid B concentrations of these dried blood spots were quantified against a standard curve with hematocrit of 55%. Acceptance criteria were mean difference to nominal value within ±15%. The relative error of all the QC samples with different hematocrit levels were within ±10.2%. The precision (%CV) for all QC measurements were < 6.5%. Therefore, dried blood spots with hemotacrit in the range of 40 to 70% can be accurately quantified with standard curve prepared with hemotacrit of 55%.

Effect of punch location

Due to chromatographic effects on the paper cards, concentration gradients may occur within the spot. As this behavior is compound dependent, it is recommended to test the influence of punch position for every new method. Sampling was performed from the peripheral areas versus center of the spot to test the effect of punch location. The difference between mean value from the center punch (n = 4) and the mean value from the peripheral punch (n = 16) was less than 4.4%. Good precisions for center punch (4.5% CV) and peripheral punch (8.85 CV) were observed. These results suggested that effect of punch location on the values was insignificant.

Stability in whole blood, dried blood spots, processed samples, stock and working solutions

The allowable time bile acid B spiked whole blood sample can remain at room temperature prior to spotting on a newborn screening card was determined with LQC and HQC blood samples, which were remained at room temperature for 27 hours prior to spotting. Three replicates were assessed and the accuracy (within ± 4.5% RE) and precision (<7.5% CV) were within the quality control acceptance criteria stated above. Bile acid B is therefore considered stable in whole blood for 27 hours prior to spotting.

The stability of bile acid B in dried blood spots on the newborn screening cards stored at room temperature and -20 ºC for 66 days and at 37 ºC for 90 hours was assessed by comparisons of three replicates of stored LQC and HQC against freshly prepared calibration standards and QC samples. The results showed the accuracy (-8.3 to 7.5% RE) and precision (≤ 6% CV) for these two levels of QC samples, indicating that dried blood spot samples were stable for at least 66 days if stored at room temperature or -20 ºC and for 90 hours under shipping conditions (37 ºC).

Processed sample stability was assessed by re-injection of LQC and HQC together with calibration curve from one accuracy/precision run after storage in the autosampler at 4 ºC for 7 days. Stability was demonstrated by accuracy (< ±5.1% RE) and precision (≤ 6% CV).

Stock solution stability of bile acid B and internal standard in acetonitrile-water (1:1) was established for 22 hours at room temperature. The internal standard in aqueous working solution (1% sodium dodecyl sulfate (SDS) and 50 mM trisodium citrate at pH 12) was stable for 12 days at room temperature.

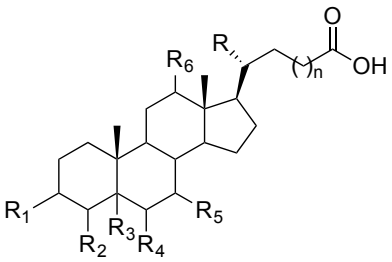

1 deoxycholic acid (DCA)
$R = CH_3$, n = 1
$R_1 = R_6$ = α-OH
$R_2 = R_4 = R_5$ = H, R_3 = β-H

2 chenodeoxycholic acid (CDCA)
$R = CH_3$, n = 1
$R_1 = R_5$ = α-OH
$R_2 = R_4 = R_6$ = H, R_3 = β-H

3 cholic acid (CA)
$R = CH_3$, n = 1
$R_1 = R_5 = R_6$ = α-OH
$R_2 = R_4$ = H, R_3 = β-H

4 α-muricholic acid
$R = CH_3$, n = 1
$R_1 = R_4 = R_5$ = α-OH
$R_2 = R_6$ = H, R_3 = β-H

5 β-muricholic acid
$R = CH_3$, n = 1
R1 = R_5 = α-OH
R_4 = β-OH
$R_2 = R_6$ = H, R_3 = β-H

6 5 -cholanic acid-3α,4β,7α-triol
$R = CH_3$, n = 1
$R_1 = R_5$ = α-OH
R_2 = β-OH
$R_4 = R_6$ = H, R_3 = β-H

7 21,26,27-trinorcholestan-25-oic acid-3β,5α,6α-triol
R = H, n = 3
$R_1 = R_4$ = β-OH, R_3 = α-OH
$R_2 = R_5 = R_6$ = H

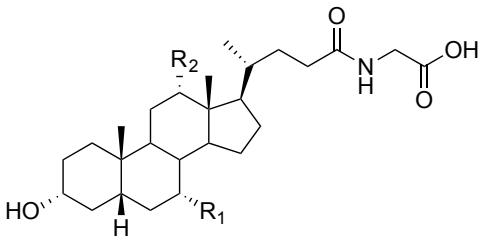

8 glycodeoxycholic acid (GDCA)
R_1 = H
R_2 = OH

9 glycochenodeoxycholic acid (GCDCA)
R_1 = OH
R_2 = H

10 glycocholic acid (GCA)
$R_1 = R_2$ = OH

Figure S1. Structures of bile acids and analog that were used to study fragmentation patterns of the AMPP derivatives

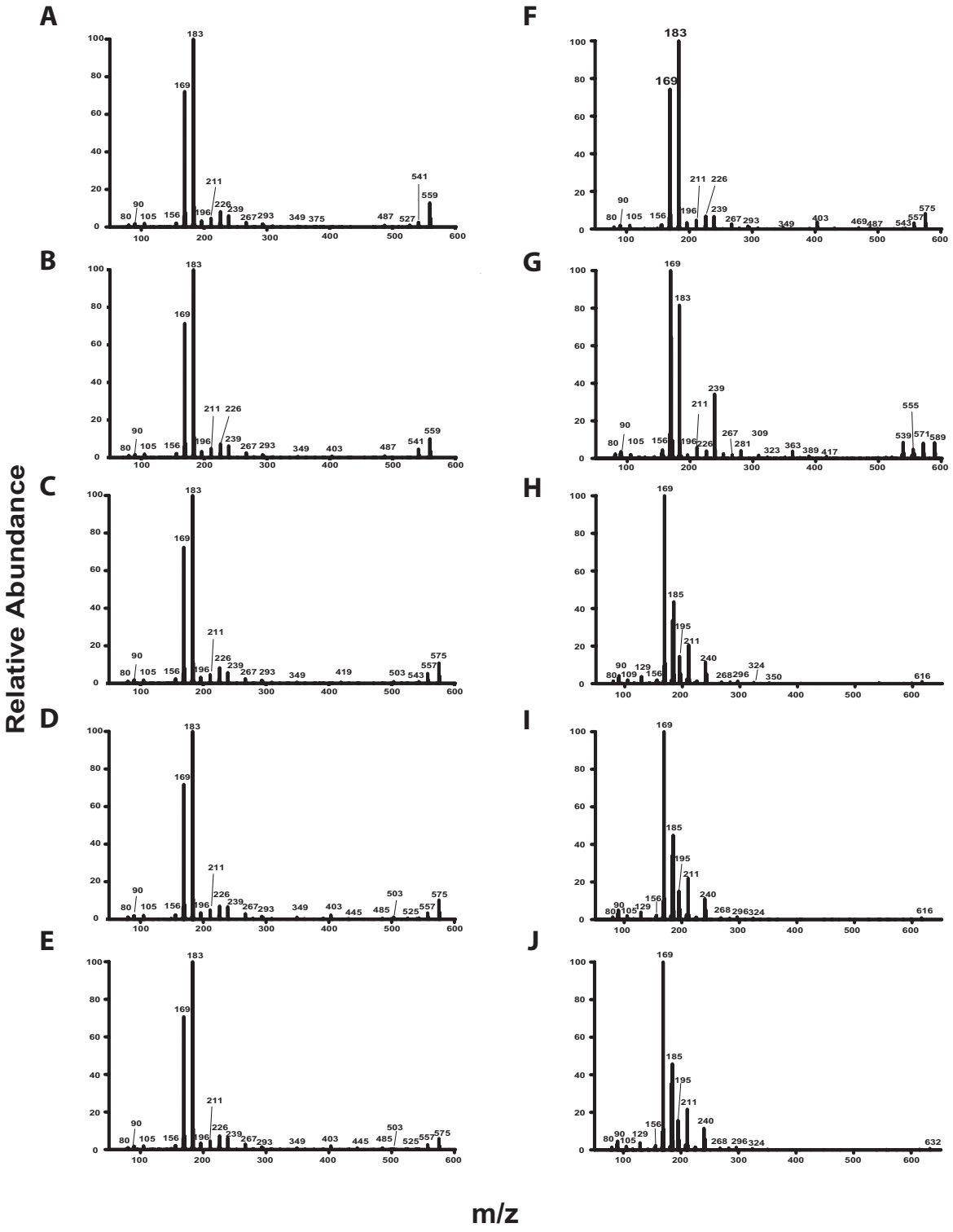

Figure S2. HCD mass spectra of AMPP-derivatized 1 (A), 2 (B), 3 (C), 4 (D), 5 (E), 6 (F), 7 (G), 8 (H), 9 (I), 10 (J).

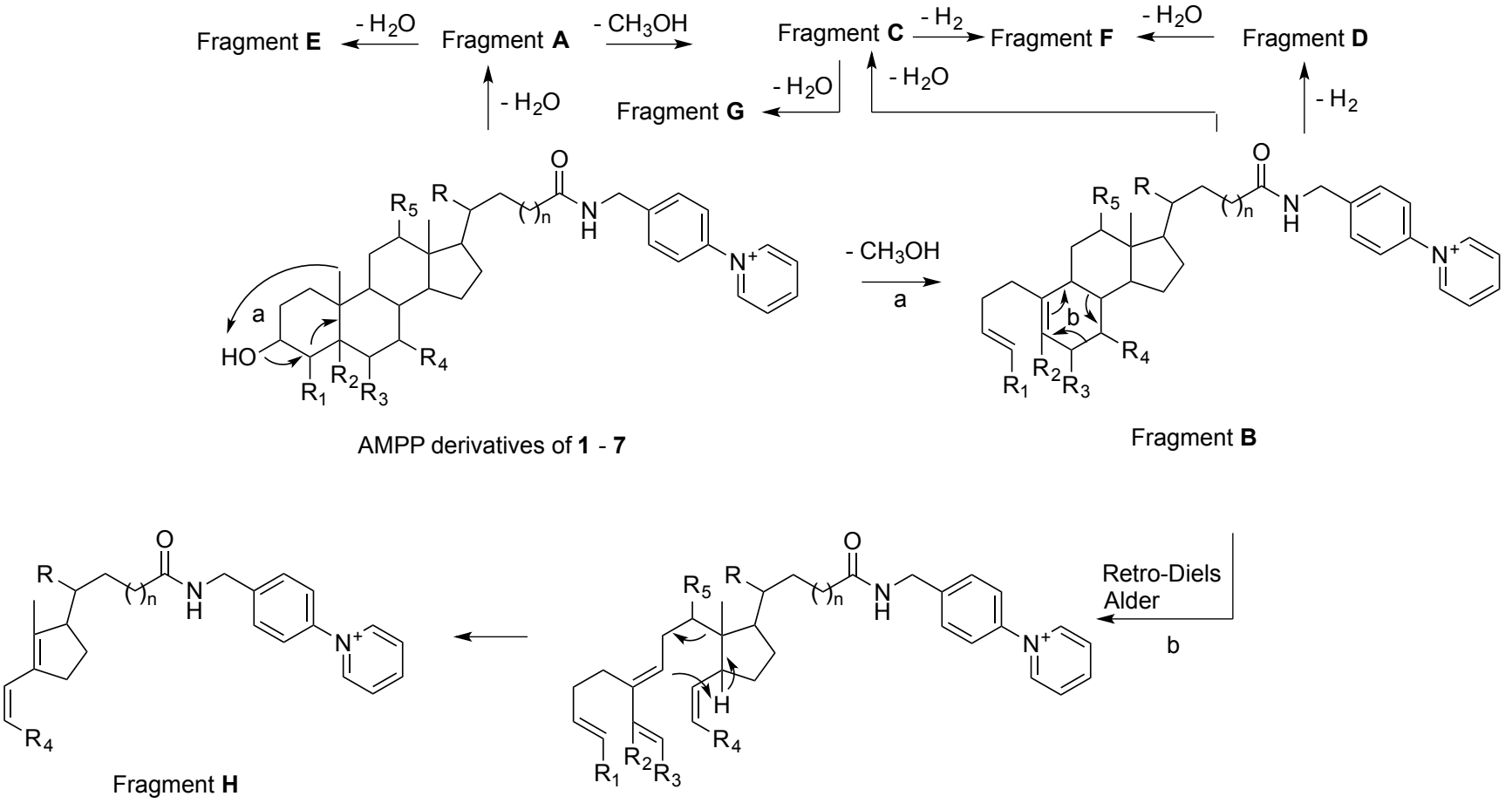

Figure S3. Proposed fragmentation pathway to fragments A – H in AMPP derivatives of unconjugated bile acids 1 – 7

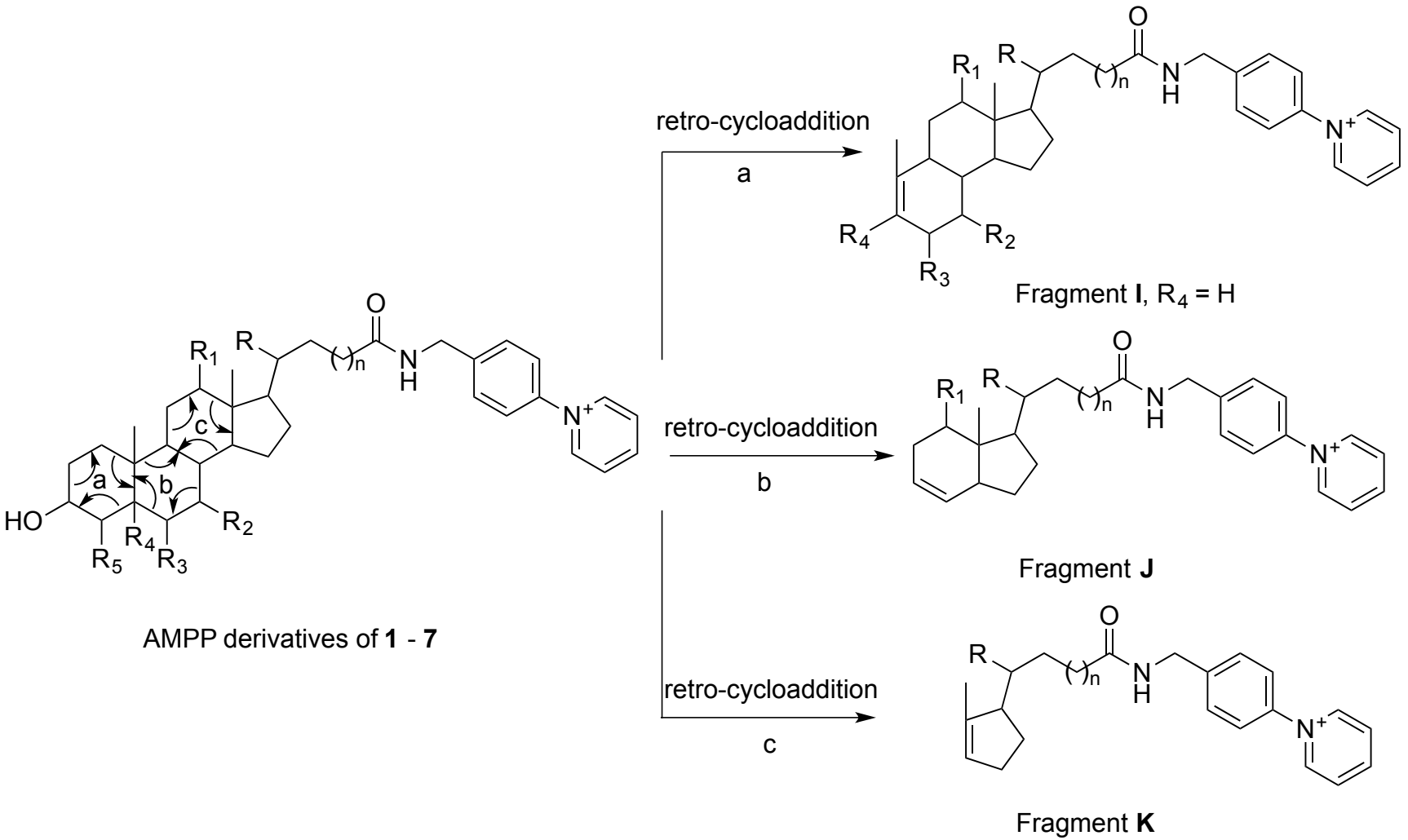

Figure S4. Proposed fragmentation pathway to fragments I – K in AMPP derivatives of unconjugated bile acids 1 – 7

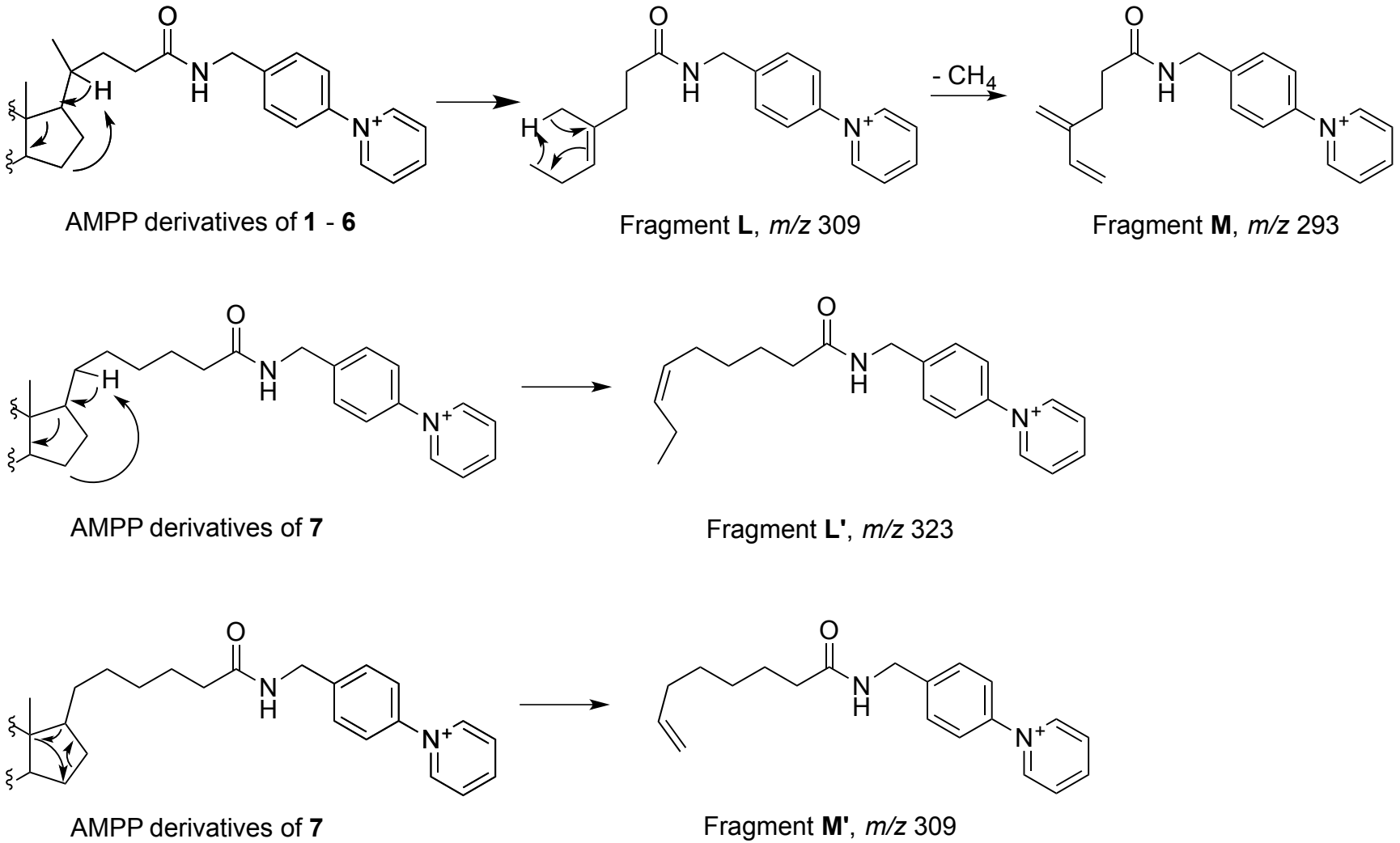

Figure S5. Proposed fragmentation pathway to fragments L (L′)– M (M′) in AMPP derivatives of unconjugated bile acids 1 – 7

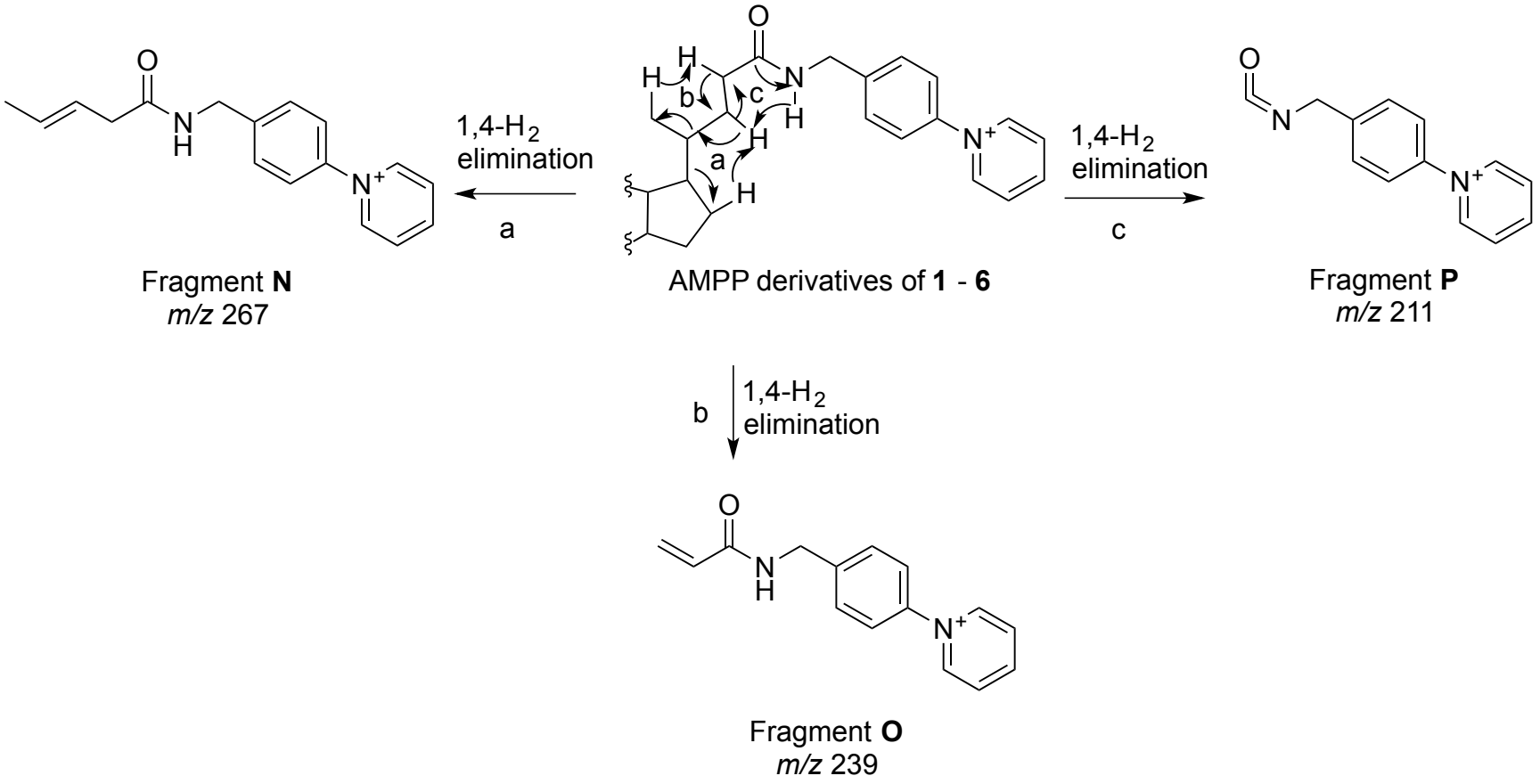

Figure S6. Proposed fragmentation pathway to fragments N – P in AMPP derivatives of unconjugated bile acids 1 – 6

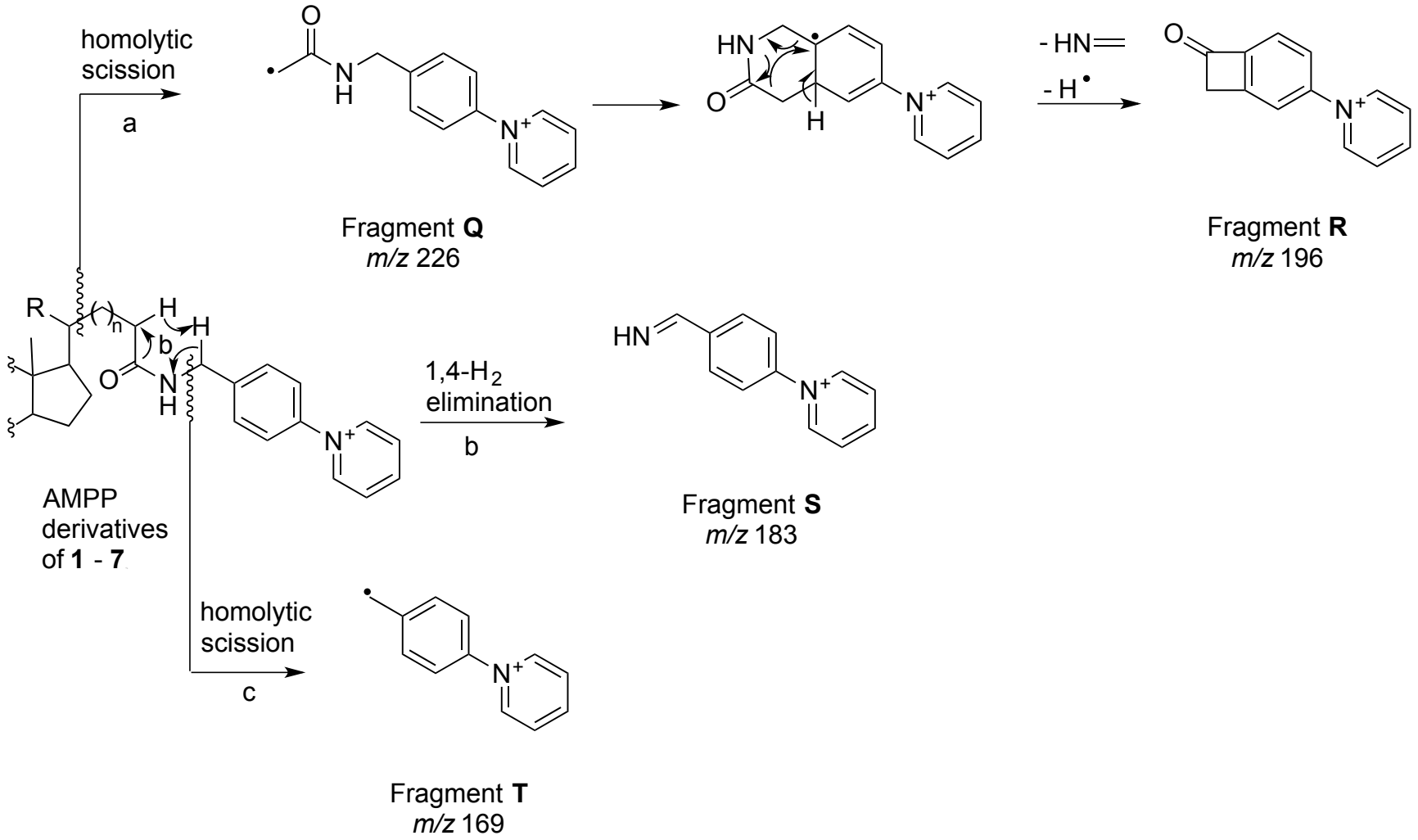

Figure S7. Proposed fragmentation pathway to fragments Q – T in AMPP derivatives of unconjugated bile acids 1 – 7

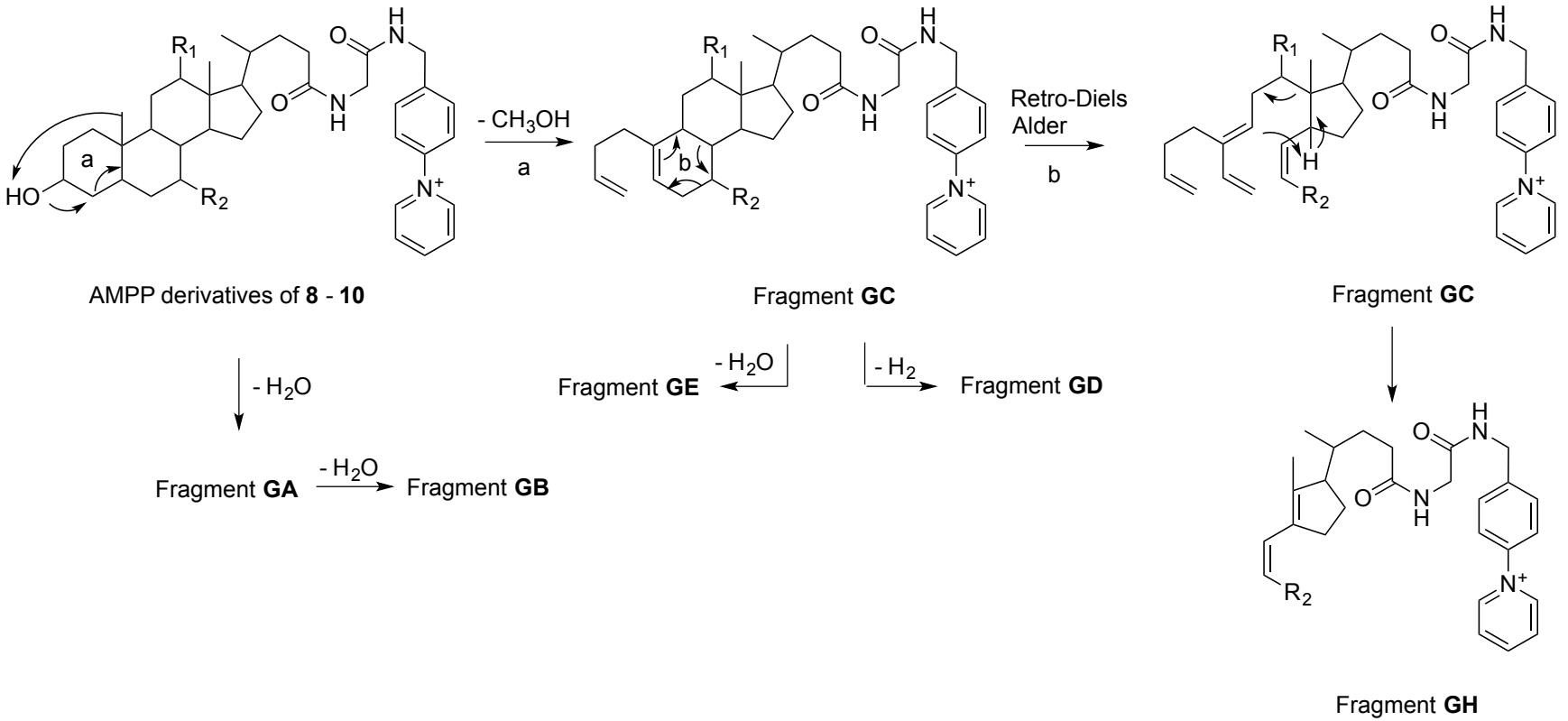

Figure S8. Proposed fragmentation pathway to fragments GA – GE, GH in AMPP derivatives of glycine conjugated bile acids 8 – 10

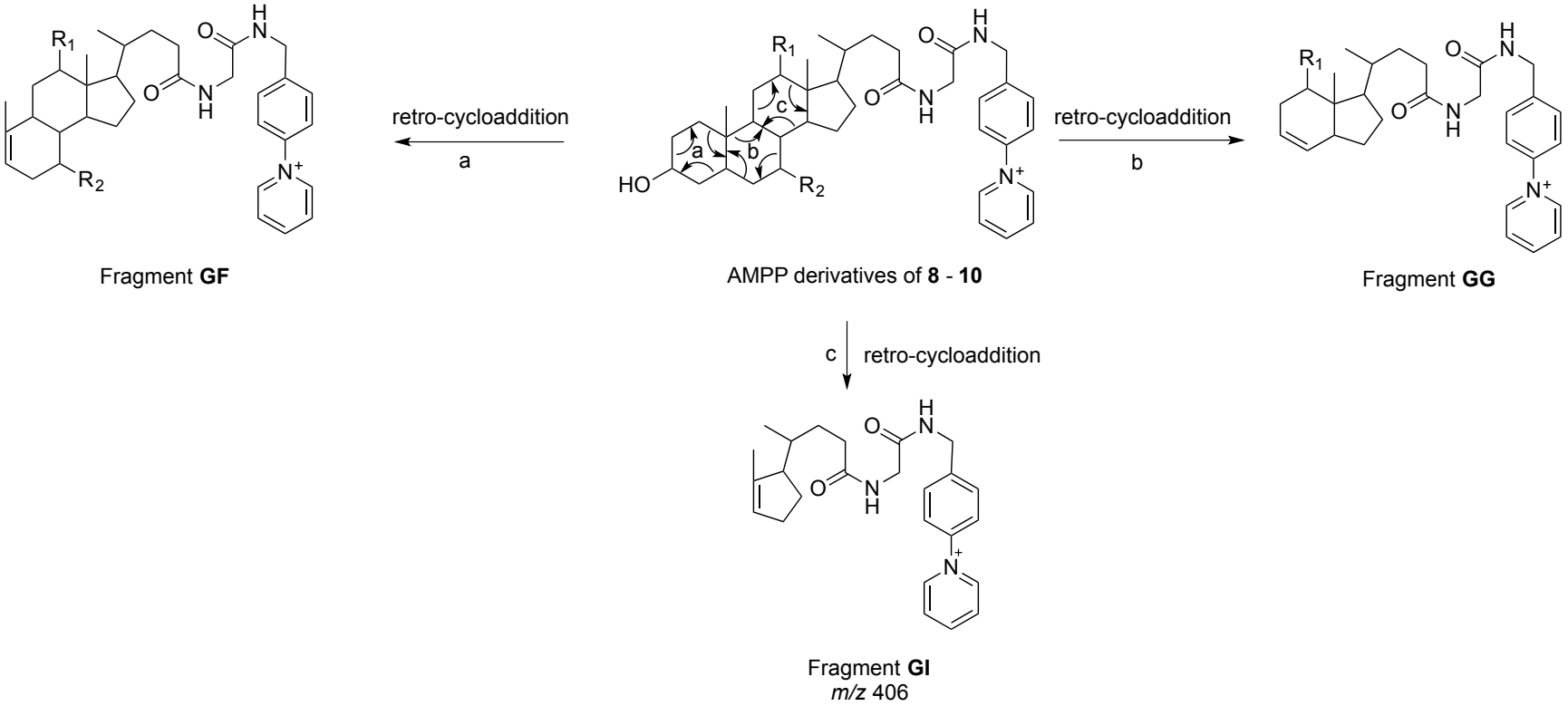

Figure S9. Proposed fragmentation pathway to fragments GF, GG, GI in AMPP derivatives of glycine conjugated bile acids 8 – 10

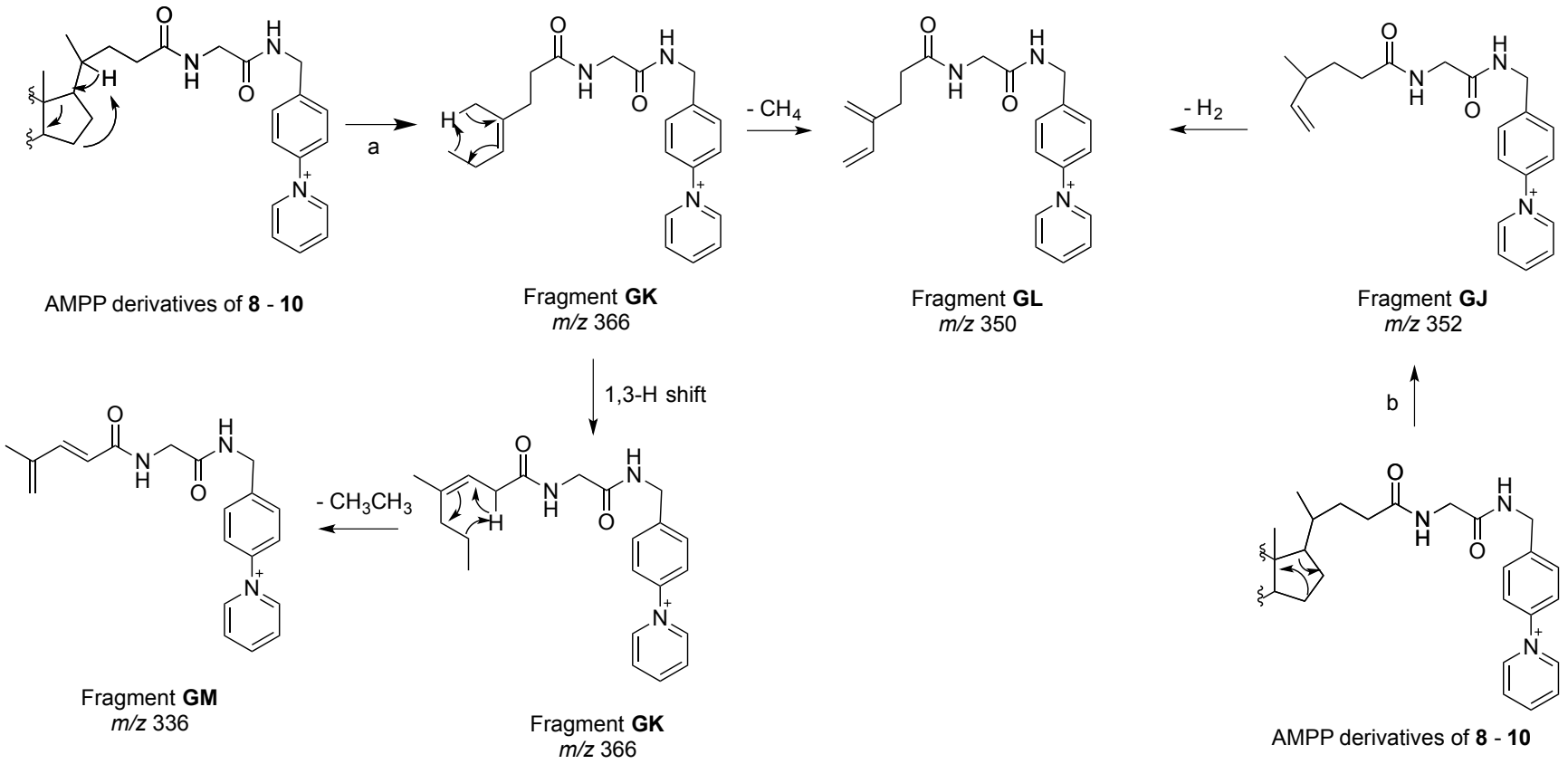

Figure S10. Proposed fragmentation pathway to fragments GJ - GM in AMPP derivatives of glycine conjugated bile acids 8 - 10

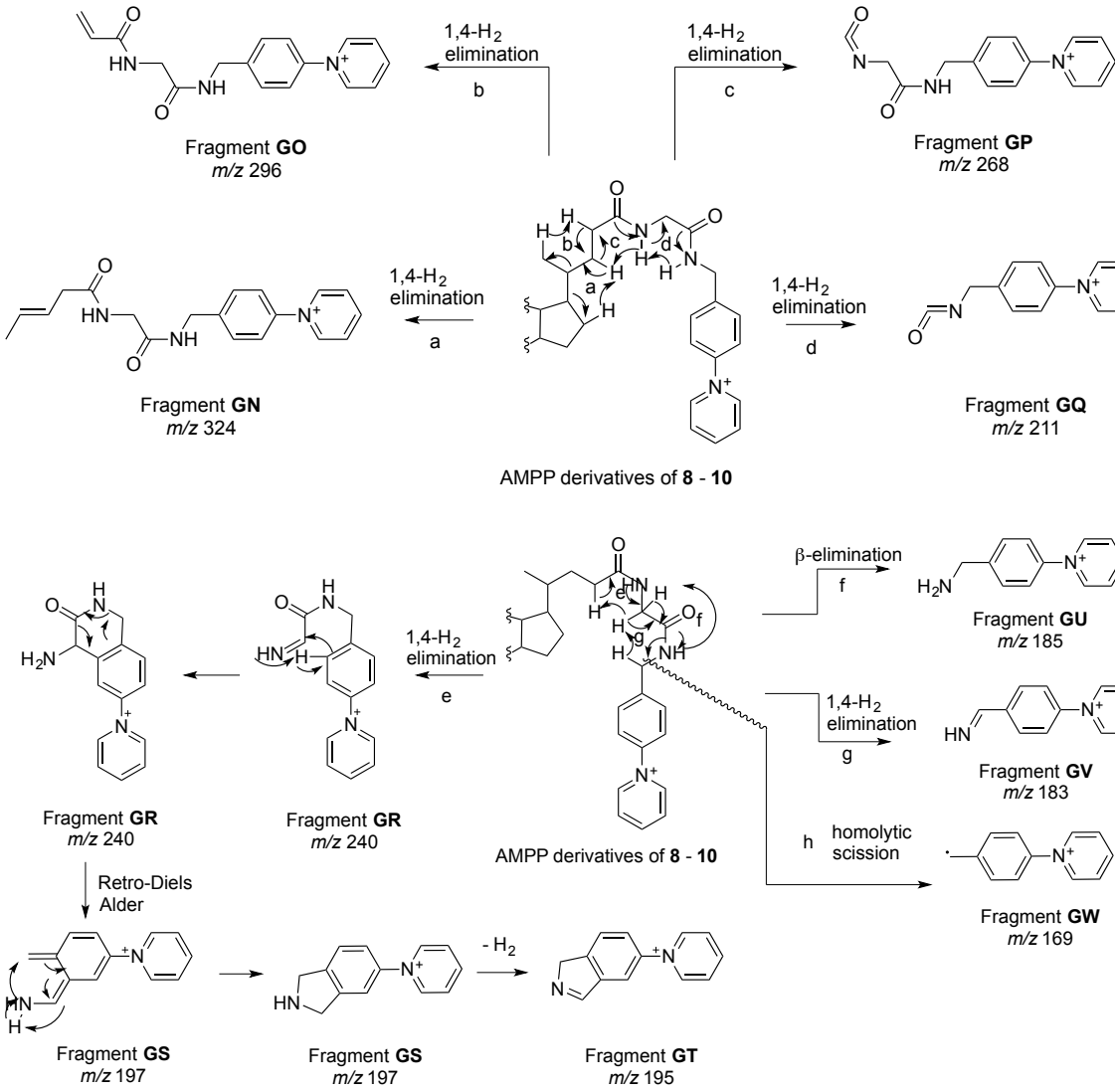

Figure S11. Proposed fragmentation pathway to fragments GN - GW in AMPP derivatives of glycine conjugated bile acids 8 – 10.

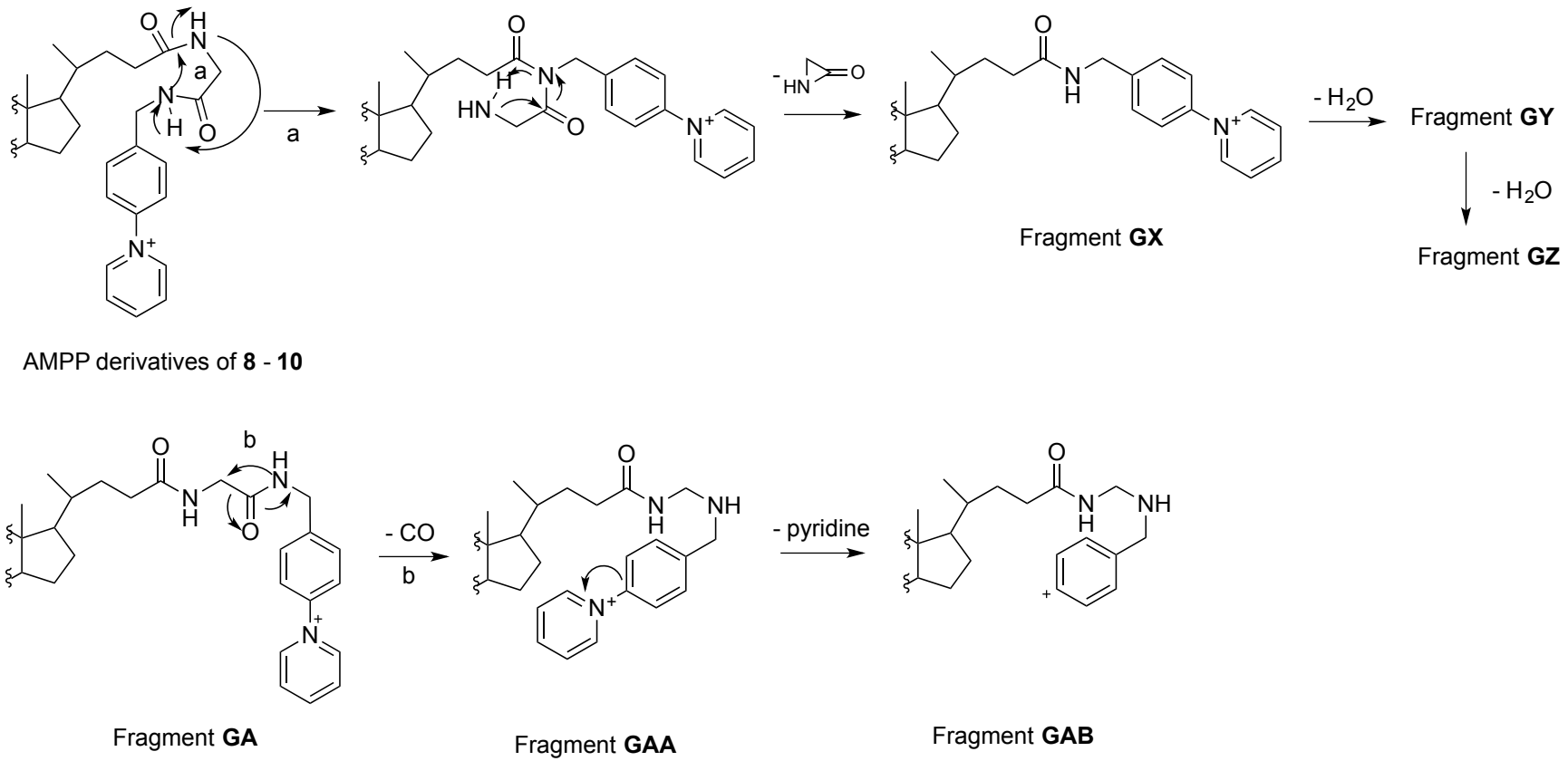

Figure S12. Proposed fragmentation pathway to fragments GX – GZ, GAA - GAB in glycine conjugated bile acid AMPP derivatives.

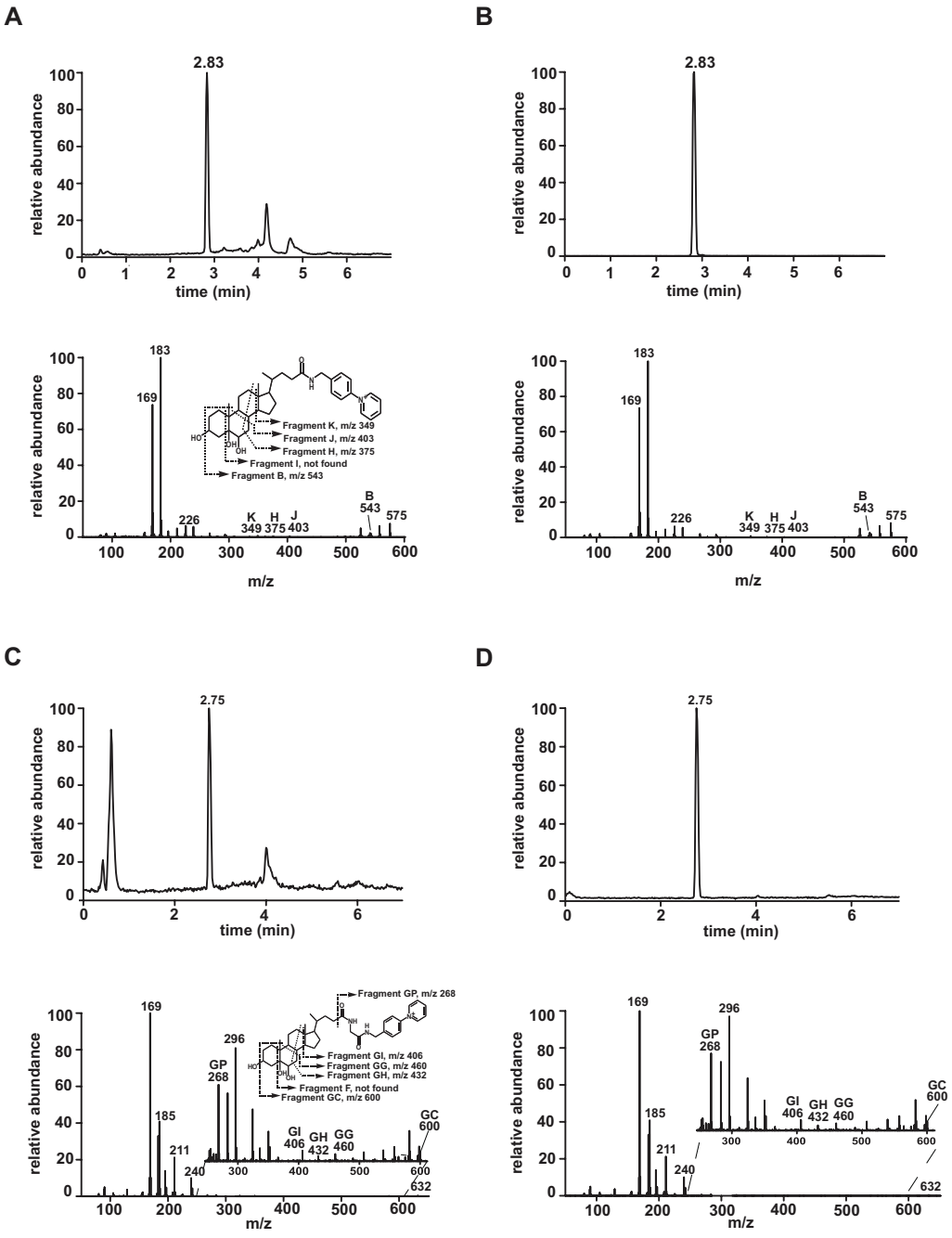

Figure S13. Comparison of chromatograms and HCD mass spectra of AMPP derivati bile acids A and B in NPC plasma and solutions of synthetic compounds Chromatograms (detected by HCD MS/MS) and HCD mass spectra of AMPP derivatives acids A in NPC1 plasma. (**B**) Chromatograms (detected by HCD MS/MS) and HCD spectra of AMPP derivatives of bile acids A in solution of synthetic compound Chromatograms (detected by HCD MS/MS) and HCD mass spectra of AMPP derivative acid B in NPC1 plasma. (**D**) Chromatograms (detected by HCD MS/MS) and HCD mass s of AMPP derivative of bile acid B in solution of synthetic compound. The key fragme AMPP derivative of bile acid A and B are also given.

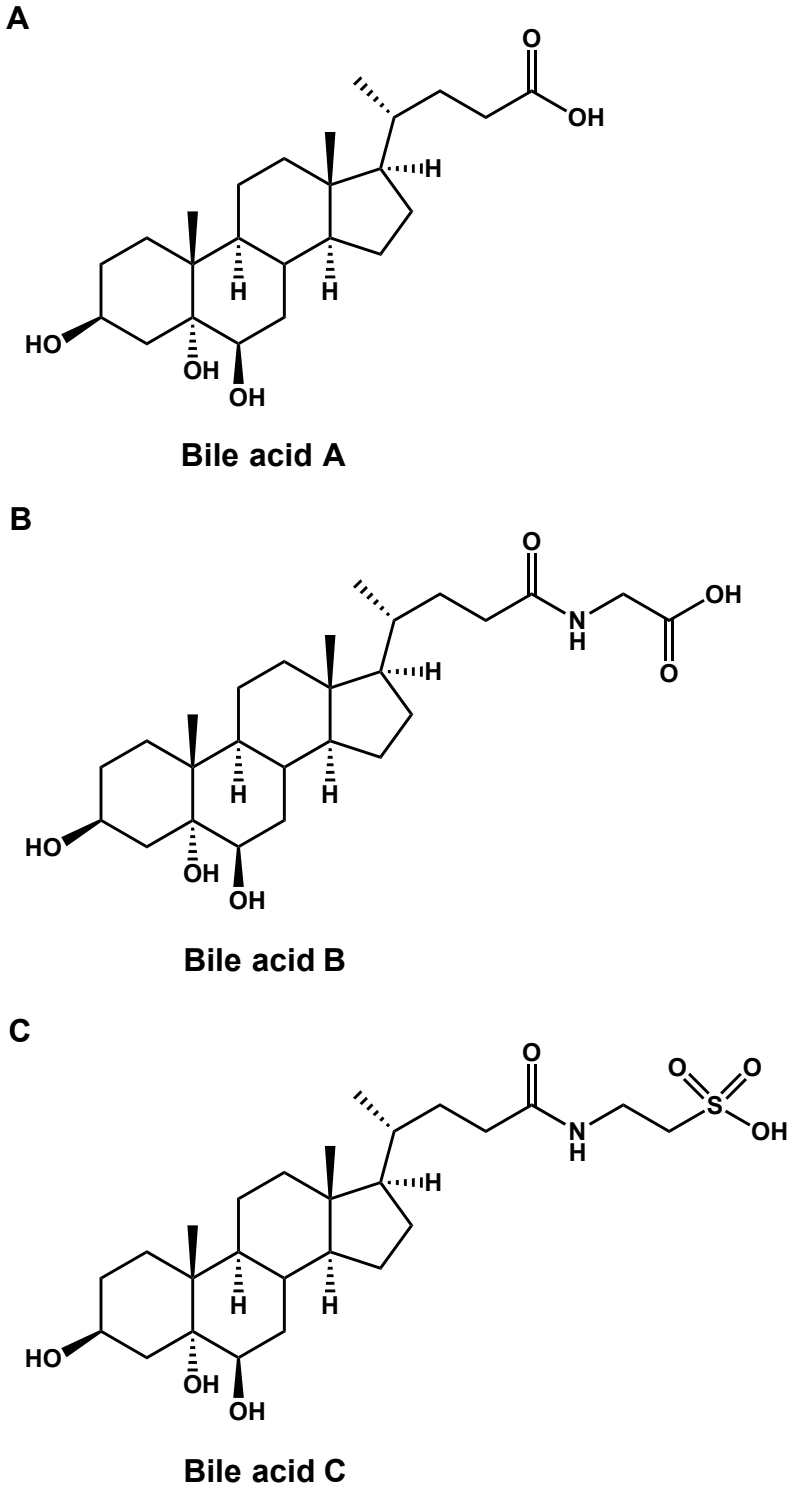

Figure S14. Structures of bile acid biomarkers for NPC. (**A**) Bile acid A, 5α-cholanic acid-3β,5α,6β-triol. (**B**) Bile acid B, 5α-cholanic acid-3β,5α,6β-triol N-(carboxymethyl)-amide. **(C)** Bile acid C, N-(3β,5α,6β-trihydroxy-cholan-24-oyl)taurine (not confirmed).

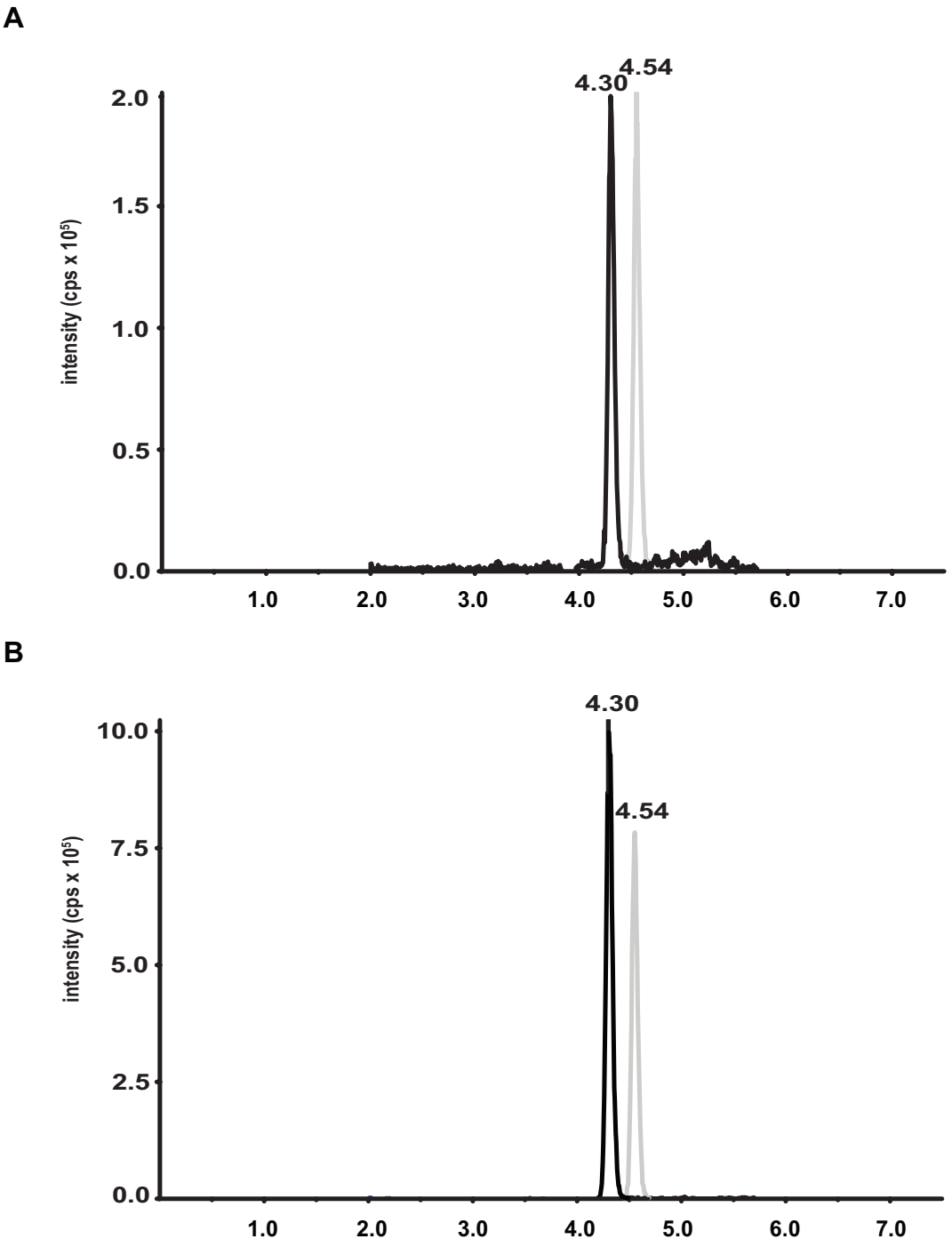

Figure S15. Comparison of chromatograms of bile acids A and B in NPC1 plasma and solutions of synthetic compounds. (**A**) Bile acids A and B in NPC1 plasma. (**B**) Bile acids A and B in solution of synthetic compounds. The bile acid was detected by MRM transition *m/z* 411 → 411at retention time of 4.30 min. The bile acid was detected by MRM transition *m/z* 464 → 74 at retention time of 4.54 min.

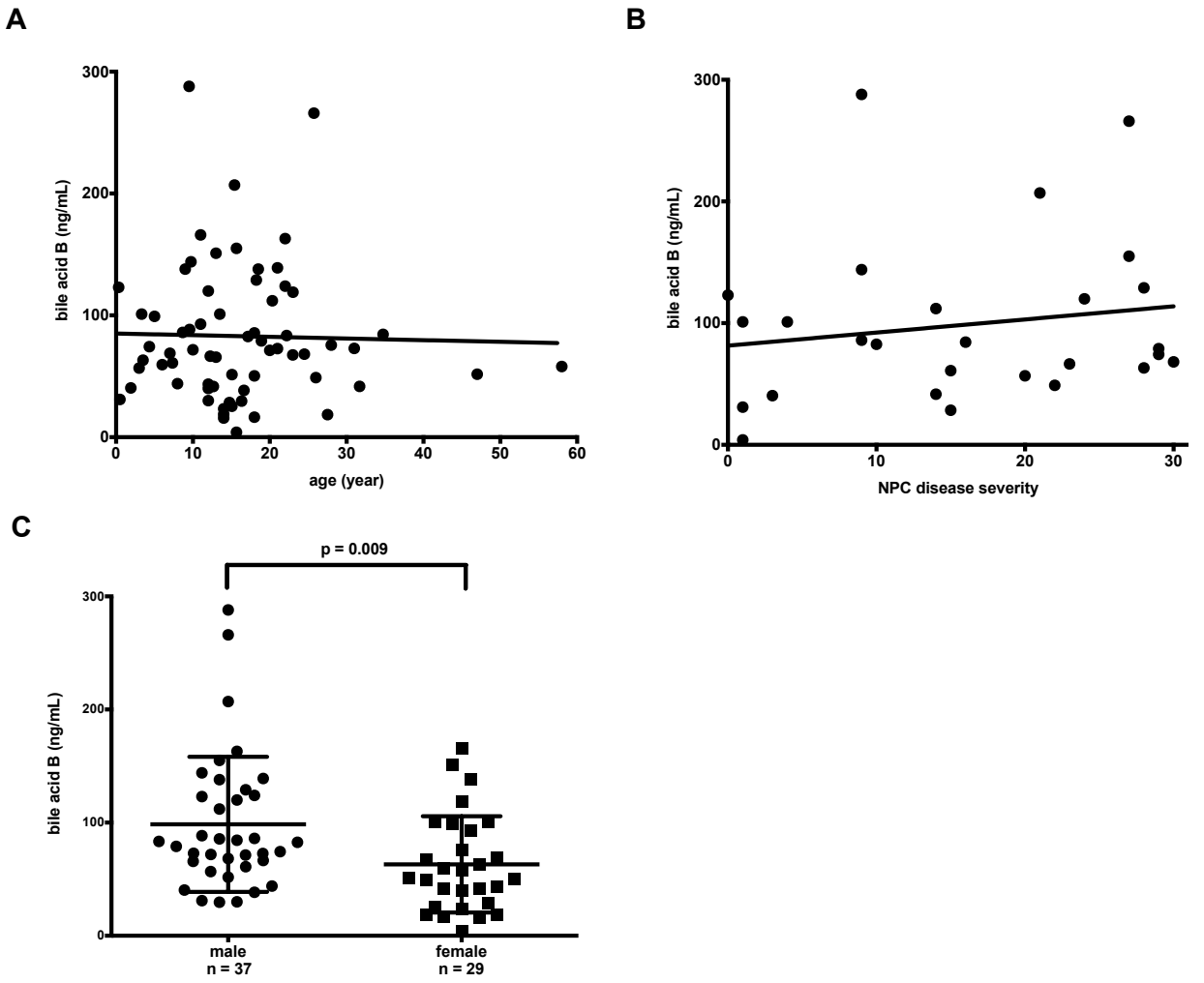

Figure S16. Correlation of bile acid B concentrations with patient parameters. (**A**) Correlation of bile acid B concentrations with age of NPC1 patients, r = -0.026, p = NS. (**B**) Correlation of bile acid B concentrations with disease severity (NPC1 disease severity scale), r = 0.16, p = NS. **(C)** Effect of gender on bile acid B concentrations in NPC1 patients, p = 0.009.

Table S1. Accurate masses and calculated elemental composition of fragment ions of 21,26,27-trinorcholestan-25-oic acid-3β,5α,6β-triol and bile acid A AMPP derivatives

Bile acid	21,26,27-trinorcholestan-25-oic acid-3β,5α,6β-triol			Bile acid A		
Fragment	Measured mass (u) (Relative intensity)	Deviation (mmu*)	Elemental composition	Measured mass (u) (Relative intensity)	Deviation (mmu*)	Elemental composition
T	169.0889 (100)	0.33	C12 H11 N	169.0889 (71.79)	0.29	C12 H11 N
S	183.092 (78.64)	0.36	C12 H11 N2	183.092 (100)	0.36	C12 H11 N2
R	196.0762 (1.86)	0.51	C13 H10 O N	196.0762 (3.32)	0.5	C13 H10 O N
P	211.0872 (5.58)	0.57	C13 H11 O N2	211.0871 (3.58)	0.53	C13 H11 O N2
Q	226.1107 (3.87)	0.61	C14 H14 O N2	226.1106 (2.57)	0.57	C14 H14 O N2
O	239.1185 (33.76)	0.59	C15 H15 O N2	239.1184 (5.4)	0.54	C15 H15 O N2
N	281.1654 (4.12)	0.53	C18 H21 O N2	267.1497 (1.69)	0.53	C17 H19 O N2
M or M′	309.1968 (1.7)	0.62	C20 H25 O N2	293.1654 (1.41)	0.6	C19 H21 O N2
L or L′	323.2123 (0.76)	0.54	C21 H27 O N2	309.1968 (0.23)	0.68	C20 H25 O N2
K	363.2437 (3.74)	0.64	C24 H31 O N2	349.2279 (0.66)	0.47	C23 H29 O N2
H	389.2594 (1.24)	0.64	C26 H33 O N2	375.2438 (0.22)	0.66	C25 H31 O N2
J	417.2907 (1.11)	0.63	C28 H37 O N2	403.2746 (0.37)	0.19	C27 H35 O N2
I	-	-	-	-	-	-
G	521.3533 (0.62)	0.66	C36 H45 O N2	507.3374 (0.31)	0.46	C35 H43 O N2
F	537.3485 (1.87)	0.92	C36 H45 O2 N2	523.3687 (0.09)	0.37	C36 H47 O N2
C	539.3641 (8.27)	0.89	C36 H47 O2 N2	525.3482 (6.17)	0.61	C35 H45 O2 N2
E	553.3798 (1.73)	0.98	C37 H49 O2 N2	539.3639 (1.43)	0.66	C36 H47 O2 N2
D	555.3589 (4.86)	0.75	C36 H47 O3 N2	541.3431 (3.51)	0.67	C35 H45 O3 N2
B	557.3745 (2.44)	0.73	C36 H49 O3 N2	543.3589 (2.35)	0.76	C35 H47 O3 N2
A	571.3903 (7.9)	0.86	C37 H51 O3 N2	557.3744 (8.9)	0.6	C36 H49 O3 N2
M+	589.4008 (8.22)	0.82	C37 H53 O4 N2	575.385 (10.87)	0.62	C36 H51 O4 N2

* 1 mmu = 0.001 Da

Table S2. Accurate masses and calculated elemental composition of fragment ions of bile acid B AMPP derivative

Bile acid	Bile acid B		
Fragment	Measured mass (u) (Relative intensity)	Deviation (mmu*)	Elemental composition
GW	169.0889 (100)	0.25	C12H11N
GV	183.0921 (33.23)	0.38	C12H11N2
GU	185.1076 (40.66)	0.31	C12H13N2
GT	195.0921 (13.68)	0.43	C13H11N2
GS	197.1078 (4.7)	0.44	C13H13N2
GQ	211.087 (21.15)	0.46	C13H11ON2
GR	240.1137 (9.86)	0.54	C14H14ON3
GP	268.1085 (0.75)	0.49	C15H14O2N3
GO	296.1398 (1.14)	0.42	C17H18O2N3
GN	324.1711 (0.51)	0.45	C19H22O2N3
GM	336.1713 (0.13)	0.6	C20H22O2N3
GL	350.1867 (0.3)	0.38	C21H24O2N3
GJ	352.2026 (0.14)	0.65	C21H26O2N3
GK	366.2181 (0.04)	0.49	C22H28O2N3
GI	406.2495 (0.1)	0.56	C25H32O2N3
GH	432.2649 (0.05)	0.34	C27H34O2N3
GG	460.2966 (0.07)	-0.62	C31H40O3
GAB	507.3587 (0.09)	0.56	C32H47O3N2
GZ	539.3639 (0.11)	0.72	C36H47O2N2
GY	557.3741 (0.14)	0.32	C36H49O3N2
GF	-	-	-
GX	575.3845 (0.04)	0.13	C36H51O4N2
GE	582.3697 (0.3)	0.71	C37H48O3N3
GAA	586.4015 (0.02)	1.17	C37H52O3N3
GB	596.3856 (0.06)	0.9	C38H50O3N3
GD	598.3647 (0.15)	0.74	C37H48O4N3
GC	600.3804 (0.09)	0.83	C37H50O4N3
GA	614.3958 (0.29)	0.57	C38H52O4N3
M+	632.4063 (0.5)	0.46	C38H54O5N3

* 1 mmu = 0.001 Da

Table S3. Accurate masses and calculated elemental composition of fragment ions of deoxycholic acid, chenodeoxycholic acid, and 5β-cholanic acid-3α,4β,7α-triol AMPP derivatives

Bile acid	Deoxycholic acid			Chemodeoxycholic acid			5β-Cholanic acid-3α,4β,7α-triol		
Fragment	Measured mass (u) (Relative intensity)	Deviation (mmu*)	Elemental composition	Measured mass (u) (Relative intensity)	Deviation (mmu*)	Elemental composition	Measured mass (u) (Relative intensity)	Deviation (mmu)	Elemental composition
T	169.0888 (73.1)	0.18	C12H11N	169.0886 (73.56)	-0.01	C12H11N	169.0885 (75.98)	-0.08	C12H11N
S	183.0919 (100)	0.18	C12H11N2	183.0917 (100)	-0.02	C12H11N2	183.0916 (100)	-0.1	C12H11N2
R	196.076 (3.31)	0.35	C13H10ON	196.0758 (3.26)	0.12	C13H10ON	196.0757 (3.27)	0.04	C13H10ON
P	211.087 (4.69)	0.4	C13H11ON2	211.0867 (4.83)	0.15	C13H11ON2	211.0867 (4.72)	0.06	C13H11ON2
Q	226.1105 (8.34)	0.42	C14H14ON2	226.1102 (7.26)	0.14	C14H14ON2	226.1101 (6.8)	0.06	C14H14ON2
O	239.1183 (6.03)	0.44	C15H15ON2	239.118 (6.37)	0.14	C15H15ON2	239.1179 (6.71)	0.05	C15H15ON2
N	267.1496 (2.33)	0.38	C17H19ON2	267.1493 (2.34)	0.07	C17H19ON2	267.1491 (2.6)	-0.04	C17H19ON2
M	293.1653 (1.6)	0.43	C19H21ON2	293.1649 (1.41)	0.09	C19H21ON2	293.1648 (1.53)	-0.02	C19H21ON2
L	309.1965 (0.6)	0.4	C20H25ON2	309.1962 (0.46)	0.01	C20H25ON2	309.1961 (0.45)	-0.05	C20H25ON2
K	349.2278 (0.44)	0.32	C23H29ON2	349.2274 (0.64)	-0.09	C23H29ON2	349.2272 (0.73)	-0.24	C23H29ON2
H	375.2433 (0.27)	0.21	C25H31ON2	391.2378 (0.31)	-0.18	C25H31O2N2	391.2377 (0.34)	-0.26	C25H31O2N2
J	419.2697 (0.16)	0.37	C27H35O2N2	403.2742 (0.64)	-0.16	C27H35ON2	403.274 (3.87)	-0.41	C27H35ON2
I	487.3323 (1)	0.42	C32H43O2N2	487.3316 (0.92)	-0.31	C32H43O2N2	487.3315 (0.6)	-0.37	C32H43O2N2
G	-	-	-	-	-	-	-	-	-
F	-	-	-	-	-	-	-	-	-
C	-	-	-	-	-	-	525.3473 (0.22)	-0.3	C35H45O2N2
E	-	-	-	523.368 (0.17)	-0.24	C36H47ON2	539.3628 (0.3)	-0.43	C36H47O2N2
D	523.3686 (0.05)	0.28	C36H47ON2	-	-	-	-	-	-
B	527.3636 (1.08)	0.37	C35H47O2N2	527.3631 (0.25)	-0.14	C35H47O2N2	543.3579 (0.45)	-0.25	C35H47O3N2
A	541.3793 (2.58)	0.44	C36H49O2N2	541.3787 (4.48)	-0.17	C36H49O2N2	557.3732 (3.38)	-0.56	C36H49O3N2
M+	559.3897 (12.86)	0.27	C36H51O3N2	559.3891 (9.99)	-0.34	C36H51O3N2	575.3838 (8.29)	-0.58	C36H51O4N2

* 1 mmu = 0.001 Da

Table S4. Accurate masses and calculated elemental composition of fragment ions of cholic acid, α-muricholic acid, and β-muricholic acid AMPP derivatives

Bile acid	Cholic_acid			α-Muricholic_acid			β-Muricholic_acid		
Fragment	Measured mass (u) (Relative intensity)	Deviation (mmu*)	Elemental composition	Measured mass (u) (Relative intensity)	Deviation (mmu*)	Elemental composition	Measured mass (u) (Relative intensity)	Deviation (mmu)	Elemental composition
T	169.0885 (73.77)	-0.11	C12H11N	169.0885 (72.21) (72.21)	-0.17	C12H11N	169.0885 (72.21)	-0.12	C12H11N
S	183.0915 (100)	-0.13	C12H11N2	183.0915 (100) (100)	-0.19	C12H11N2	183.0915 (100)	-0.15	C12H11N2
R	196.0757 (3.25)	0	C13H10ON	196.0757 (3.5) (3.5)	-0.06	C13H10ON	196.0757 (3.5)	-0.01	C13H10ON
P	211.0866 (4.67)	0.03	C13H11ON2	211.0866 (4.62) (4.62)	-0.05	C13H11ON2	211.0866 (4.62)	0.01	C13H11ON2
Q	226.1101 (8.35)	0.02	C14H14ON2	226.1101 (7.37) (7.37)	-0.06	C14H14ON2	226.1101 (7.37)	-0.01	C14H14ON2
O	239.1179 (5.76)	0.01	C15H15ON2	239.1179 (6.33) (6.33)	-0.07	C15H15ON2	239.1179 (6.33)	-0.01	C15H15ON2
N	267.1491 (2.33)	-0.09	C17H19ON2	267.1491 (2.77) (2.77)	-0.18	C17H19ON2	267.1491 (2.77)	-0.12	C17H19ON2
M	293.1648 (1.53)	-0.07	C19H21ON2	293.1647 (1.36) (1.36)	-0.18	C19H21ON2	293.1647 (1.36)	-0.1	C19H21ON2
L	309.196 (0.65)	-0.15	C20H25ON2	309.1959 (0.38) (0.38)	-0.27	C20H25ON2	309.1959 (0.38)	-0.19	C20H25ON2
K	349.2272 (0.62)	-0.25	C23H29ON2	349.2271 (0.93) (0.93)	-0.4	C23H29ON2	349.2271 (0.93)	-0.32	C23H29ON2
H	391.2377 (0.3)	-0.31	C25H31O2N2	391.2376 (0.29) (0.29)	-0.46	C25H31O2N2	391.2376 (0.29)	-0.43	C25H31O2N2
J	419.2689 (0.5)	-0.42	C27H35O2N2	403.2739 (2) (2)	-0.62	C27H35ON2	403.2739 (2)	-0.5	C27H35ON2
I	503.3264 (0.94)	-0.41	C32H43O3N2	503.3264 (0.43) (0.43)	-0.6	C32H43O3N2	503.3264 (0.43)	-0.45	C32H43O3N2
G	-	-	-	507.3364 (0.14) (0.14)	-0.85	C35H43ON2	507.3364 (0.14)	-0.6	C35H43ON2
F	-	-	-	523.3315 (0.1) (0.1)	-0.81	C35H43O2N2	523.3315 (0.1)	-0.43	C35H43O2N2
C	525.3471 (0.11)	-0.48	C35H45O2N2	525.347 (0.47) (0.47)	-0.66	C35H45O2N2	525.347 (0.47)	-0.53	C35H45O2N2
E	539.3628 (0.36)	-0.36	C36H47O2N2	539.3627 (0.44) (0.44)	-0.63	C36H47O2N2	539.3627 (0.44)	-0.48	C36H47O2N2
D	541.3419 (0.06)	-0.58	C35H45O3N2	541.3418 (0.07) (0.07)	-0.91	C35H45O3N2	541.3418 (0.07)	-0.64	C35H45O3N2
B	543.3577 (0.98)	-0.4	C35H47O3N2	543.3575 (0.31) (0.31)	-0.7	C35H47O3N2	543.3575 (0.31)	-0.58	C35H47O3N2
A	557.3731 (5.43)	-0.62	C36H49O3N2	557.373 (2.68) (2.68)	-0.85	C36H49O3N2	557.373 (2.68)	-0.72	C36H49O3N2
M+	575.3837 (10.87)	-0.61	C36H51O4N2	575.3836 (5.92) (5.92)	-0.8	C36H51O4N2	575.3836 (5.92)	-0.7	C36H51O4N2

* 1 mmu = 0.001 Da

Table S5. Accurate masses and calculated elemental composition of fragment ions of glycocholic acid, glycochenodeoxycholic acid, and glycodeoxycholic acid AMPP derivatives

Bile acid	Glycocholic_acid			Glycochenodeoxycholic_acid			Glycodeoxycholic_acid		
Fragment	Measured mass (u) (Relative intensity)	Deviation (mmu*)	Elemental composition	Measured mass (u) (Relative intensity)	Deviation (mmu*)	Elemental composition	Measured mass (u) (Relative intensity)	Deviation (mmu)	Elemental composition
GW	169.0885 (100)	-0.15	C12H11N	169.0889 (100)	0.28	C12H11N	169.0884 (100)	-0.2	C12H11N
GV	183.0917 (34.37)	-0.02	C12H11N2	183.0921 (33.33)	0.45	C12H11N2	183.0916 (33.79)	-0.06	C12H11N2
GU	185.1072 (44.28)	-0.12	C12H13N2	185.1077 (43.1)	0.35	C12H13N2	185.1072 (42.8)	-0.17	C12H13N2
GT	195.0917 (15.1)	-0.01	C13H11N2	195.0922 (14.51)	0.48	C13H11N2	195.0916 (14.19)	-0.06	C13H11N2
GS	197.1073 (5.09)	-0.01	C13H13N2	197.1078 (5.19)	0.49	C13H13N2	197.1073 (5.03)	-0.05	C13H13N2
GQ	211.0866 (20.95)	-0.02	C13H11ON2	211.0871 (21.18)	0.52	C13H11ON2	211.0865 (20.39)	-0.06	C13H11ON2
GR	240.1131 (11.11)	0.01	C14H14ON3	240.1138 (10.68)	0.62	C14H14ON3	240.1131 (11.2)	-0.04	C14H14ON3
GP	268.108 (0.79)	-0.09	C15H14O2N3	268.1086 (0.79)	0.59	C15H14O2N3	268.1079 (0.76)	-0.12	C15H14O2N3
GO	296.1391 (1.19)	-0.25	C17H18O2N3	296.1398 (1.27)	0.49	C17H18O2N3	296.1391 (1.16)	-0.25	C17H18O2N3
GN	324.1704 (0.61)	-0.27	C19H22O2N3	324.1712 (0.59)	0.57	C19H22O2N3	324.1703 (0.57)	-0.32	C19H22O2N3
GM	336.1703 (0.09)	-0.31	C20H22O2N3	336.1714 (0.14)	-0.61	C22H24O3	336.1704 (0.08)	-0.21	C20H22O2N3
GL	350.186 (0.33)	-0.26	C21H24O2N3	350.1869 (0.32)	0.64	C21H24O2N3	350.186 (0.36)	-0.33	C21H24O2N3
GJ	352.2018 (0.2)	-0.18	C21H26O2N3	352.2026 (0.16)	-0.65	C23H28O3	352.2016 (0.18)	-0.36	C21H26O2N3
GK	366.2173 (0.08)	-0.35	C22H28O2N3	366.2183 (0.07)	0.65	C22H28O2N3	366.2172 (0.07)	-0.36	C22H28O2N3
GI	406.2485 (0.11)	-0.44	C25H32O2N3	406.2496 (0.12)	0.66	C25H32O2N3	406.2484 (0.09)	-0.5	C25H32O2N3
GH	448.2593 (0.05)	-0.19	C27H34O3N3	448.2601 (0.05)	0.56	C27H34O3N3	432.2638 (0.04)	-0.75	C27H34O2N3
GG	476.2903 (0.07)	-0.47	C29H38O3N3	460.2966 (0.1)	-0.59	C31H40O3	476.2902 (0.03)	-0.62	C29H38O3N3
GAB	507.3575 (0.03)	-0.64	C32H47O3N2	491.3641 (0.15)	0.88	C32H47O2N2	491.363 (0.03)	-0.23	C32H47O2N2
GZ	539.3625 (0.05)	-0.73	C36H47O2N2	523.3691 (0.06)	0.83	C36H47ON2	523.3676 (0.05)	-0.68	C36H47ON2
GY	557.3731 (0.2)	-0.66	C36H49O3N2	541.3799 (0.27)	1.01	C36H49O2N2	541.3783 (0.27)	-0.57	C36H49O2N2
GF	560.3477 (0.07)	-0.63	C34H46O4N3	544.3546 (0.09)	-0.09	C36H48O4	544.353 (0.1)	-0.39	C34H46O3N3
GX	575.3839 (0.05)	-0.48	C36H51O4N2	559.3903 (0.06)	0.9	C36H51O3N2	559.3889 (0.07)	-0.55	C36H51O3N2
GE	582.3677 (0.01)	-1.31	C37H48O3N3	-	-	-	570.4049 (0.03)	-0.52	C37H52O2N3
GAA	586.3994 (0.03)	-0.93	C37H52O3N3	570.4065 (0.03)	1.06	C37H52O2N3	584.3842 (0.12)	-0.5	C37H50O3N3
GB	596.3841 (0.03)	-0.61	C38H50O3N3	-	-	-	-	-	-
GD	-	-	-	584.3851 (0.03)	0.46	C37H50O3N3	-	-	-
GC	600.379 (0.09)	-0.62	C37H50O4N3	580.391 (0.01)	1.25	C38H50O2N3	-	-	-
GA	614.3944 (0.34)	-0.83	C38H52O4N3	598.4014 (0.39)	1.07	C38H52O3N3	598.3996 (0.27)	-0.71	C38H52O3N3
M+	632.4049 (0.73)	-0.95	C38H54O5N3	616.4116 (0.89)	0.72	C38H54O4N3	616.4099 (1.08)	-0.97	C38H54O4N3

* 1 mmu = 0.001 Da

Table S6. MRM transitions and MS parameters for bile acids in the first-tier biomarker screening

Q1	Q3	ID	DP	CE
407.3	407.3	CA	100	35
391.3	391.3	CDCA/DCA/UDCA/HDCA	100	35
375.3	375.3	LCA	100	35
464.3	74	GCA	90	72
448.3	74	GCDCA/GDCA/GUDCA/GHDCA	85	70
432.3	74	GLCA	85	70
514.3	80	TCA	140	116
498.3	80	TCDCA/TDCA/TUDCA/THDCA	140	116
482.3	80	TLCA	140	116
444.3	74	B^-ol-one-G	90	70
460.3	74	B^-diol-one-G	90	70
462.3	74	B-diol-one-G	90	70
467.3	97	B^-ol-one-S-1	90	70
233.1	97	B^-ol-one-S-2	80	70
469.3	97	B^-diol-one-S-1	90	70
234.1	97	B^-diol-one-S-2	80	70
480.3	74	B-tetrol-G	90	70
494.3	80	B^-ol-one-T	140	116
510.3	80	B^-diol-one-T	140	116
510.3	97	B^-ol-G-S-1	90	70
510.3	74	B^-ol-G-S-2	90	70
254.7	97	B^-ol-G-S-3	80	70
254.7	74	B^-ol-G-S-4	80	70
512.3	80	B-diol-one-T	140	116
524.4	97	B^-ol-one-G-S-1	90	70
524.4	74	B^-ol-one-G-S-2	90	70
261.7	97	B^-ol-one-G-S-3	80	70
261.7	74	B^-ol-one-G-S-4	80	70
526.4	97	B^-diol-G-S-1	90	70
526.4	74	B^-diol-G-S-2	90	70
262.7	97	B^-diol-G-S-3	80	70
262.7	74	B^-diol-G-S-4	80	70
528.4	97	B-diol-G-S-1	90	70
528.4	74	B-diol-G-S-2	90	70
263.7	97	B-diol-G-S-3	80	70
263.7	74	B-diol-G-S-4	80	70
530.4	80	B-tetrol-T	140	116
544.4	97	B-triol-G-T-1	90	70
544.4	74	B-triol-G-T-2	90	70
271.6	97	B-triol-G-T-3	80	70
271.6	74	B-triol-G-T-4	80	70
279.6	80	B^-ol-T-S-1	140	116
279.6	97	B^-ol-T-S-2	80	70
286.7	80	B^-ol-one-T-S-1	140	116
286.7	97	B^-ol-one-T-S-2	80	70
287.7	80	B^-diol-T-S-1	140	116
287.7	97	B^-diol-T-S-2	80	70
288.7	80	B-diol-T-S-1	140	116
288.7	97	B-diol-T-S-2	80	70

CA: cholic acid; CDCA: chenodeoxycholic acid; DCA: deoxycholic acid; LCA: lithocholic acid; UDCA : ursodeoxycholic acid; HDCA, hyodeoxycholic a taurocholic acid; TCDCA : taurochenodeoxycholic acid; TDCA: taurodeoxycholic acid; TLCA: taurolithocholic acid; TUDCA: tauroursodeoxycholic a glycocholic acid; GCDCA: glycochenodeoxycholic acid; GDCA: glycodeoxycholic acid; GLCA: glycolithocholic acid; GUDCA: glycoursodeoxycl GHDCS, glycoyodeoxycholic acid, B: cholanoic acid; ^: double bond; G: glycine; T: taurine; S: sulfate

Table S7. MRM transitions and MS parameters for bile acids in the second-tier biomarker screening

Q1	Q3	ID	DP	CE
407.3	407.3	CA	-120	-35
391.3	391.3	CDCA/DCA/UDCA/HDCA	-120	-35
375.3	375.3	LCA	-150	-35
464.3	74	GCA	-120	-72
448.3	74	GCDCA/GDCA/GUDCA/GHDCA	-120	-70
432.3	74	GLCA	-120	-70
514.3	80	TCA	-150	-120
498.3	80	TCDCA/TDCA/TUDCA/THDCA	-150	-120
482.3	80	TLCA	-150	-120
444.3	74	B^-ol-one-G	-90	-70

CA: cholic acid; CDCA: chenodeoxycholic acid; DCA: deoxycholic acid; LCA: lithocholic acid; UDCA : ursodeoxycholic acid; HDCA, hyodeoxycholic acid; TCA : taurocholic acid; TCDCA : taurochenodeoxycholic acid; TDCA: taurodeoxycholic acid; TLCA: taurolithocholic acid; TUDCA: tauroursodeoxycholic acid; GCA: glycocholic acid; GCDCA: glycochenodeoxycholic acid; GDCA: glycodeoxycholic acid; GLCA: glycolithocholic acid; GUDCA: glycoursodeoxycholic acid; GHDCS, glycoyodeoxycholic acid, B: cholanoic acid; ^: double bond; G: glycin

Table S8. Accuracy and precision of QC samples

Analytical Batch Number	Assay	First-tier assay					Second-tier assay				
	QC level	LLOQ	LLQC	LQC	MQC	HQC	LLOQ	LLQC	LQC	MQC	HQC
	Nominal concentration	5 ng/mL	10 ng/mL	30 ng/mL	150 ng/mL	300 ng/mL	5 ng/mL	10 ng/mL	30 ng/mL	150 ng/mL	300 ng/mL
1	Intra-run Mean	4.61	9.36	28.3	155	308	4.92	9.59	29.0	151	314
	Intra-run %CV	6.03	4.34	7.89	7.25	5.27	7.68	6.09	9.99	5.78	7.25
	Intra-run %RE	-7.87	-6.45	-5.83	3.22	2.63	-1.60	-4.07	-3.43	0.70	4.43
	n	6	6	6	6	6	6	6	6	6	6
2	Intra-run Mean	5.33	9.44	28.9	153	300	5.75	10.32	26.1	147	294
	Intra-run %CV	9.22	5.90	6.48	3.67	5.10	9.17	8.68	8.54	7.02	7.01
	Intra-run %RE	6.73	-5.65	-3.70	2.27	0.03	14.90	3.22	-13.22	-2.30	-1.98
	n	6	6	6	6	6	6	6	6	6	6
3	Intra-run Mean	5.33	9.13	26.2	146	290	5.62	9.38	28.0	149	289
	Intra-run %CV	7.27	4.04	6.61	5.29	7.96	3.71	6.18	5.43	2.70	11.76
	Intra-run %RE	6.53	-8.68	-12.55	-2.85	-3.35	12.33	-6.41	-6.60	-1.82	-1.45
	n	6	6	6	6	6	6	6	6	6	6
Inter-batch	Inter-run Mean	5.09	9.31	27.8	151	299	5.43	9.76	27.7	149	299
	Inter- run %CV	9.99	4.77	7.89	6.08	6.33	9.69	7.99	8.97	5.27	9.07
	Inter- run %RE	1.79	-6.93	-7.31	0.81	-0.22	8.54	-2.36	-7.76	-0.89	-0.37
	n	18	18	18	18	18	18	18	18	18	18